Best Practices for Mitigating Irreversible Capacity Loss of Negative Electrodes in Li-Ion Batteries

Vanchiappan Aravindan, Yun-Sung Lee, and Srinivasan Madhavi**

Development of high performance lithium-ion (Li-ion) power packs is a topic receiving significant attention in research today. Future development of the Li-ion power packs relies on the development of high capacity and high rate anodes. More specifically, materials undergo either conversion or an alloying mechanism with Li. However, irreversible capacity loss (ICL) is one of the prime issues for this type of negative electrode. Traditional insertion-type materials also experience ICL, but it is considered negligible. Therefore, eliminating ICL is crucial before the fabrication of practical Li-ion cells with conventional cathodes such as $LiFePO_4$, $LiMn_2O_4$, etc. There are numerous methods for eliminating ICL such as pre-treating the electrode, usage of stabilized Li metal powder, chemical and electrochemical lithiation, sacrificial salts for both anode and cathode, etc. The research strategies that have been explored are reviewed here in regards to the elimination of ICL from the high capacity anodes as described. Additionally, mitigating ICL observed from the carbonaceous anodes is discussed and compared.

1. Introduction

The lithium-ion battery (LIB) is one of the prominent electrochemical energy storage systems currently available owing to its high energy density (both volumetric and gravimetric), long calendar life, maintenance free nature, low self-discharge, flexibility, and shape versatility.[1–11] Therefore, the LIB completely dominates the electronic appliances market. Attempts have also been made to exploit the LIB for zero emission transportation applications such as hybrid electric vehicles (HEV) and electric vehicles (EV) as well as grid storage.[12,13] Commercial LIBs are composed of graphite for the anode and layered $LiCoO_2$ or olivine-type $LiFePO_4$ for the cathode in the presence of an aprotic organic solvent. Poor rate capability, limited capacity (theoretical capacity of ≈372 mA h g^{-1}), Li-plating issues, irreversible electrolyte decomposition in the first cycle, and subsequent solid electrolyte interphase (SEI) formation certainly offset the possible usage in high power Li-ion power packs.[5] Therefore, intense research activity has been carried out to replace the conventional graphitic anodes.

Unfortunately, insertion type materials such as oxides, sulfides, and phosphates offer a higher working potential (>1 V vs Li), and decent practical capacity compared to graphite, which certainly dilutes the net energy density of the cell. For instance, $Li_4Ti_5O_{12}$, the anatase and bronze phases of TiO_2, $LiCrTiO_4$, Nb_2O_5, $TiNb_2O_7$, TiP_2O_7, $LiTi_2(PO_4)_3$ etc., have been extensively evaluated.[5,7,14] Spinel $Li_4Ti_5O_{12}$, which is commercially available, utilizes a $LiMn_2O_4$ cathode for HEV and EV applications, although it offers low theoretical energy density (≈200 W h kg^{-1}).[13] Apart from the insertion, the emergence of high capacity, high power alloy and conversion (often called displacement) type materials has attracted widespread attention in the last two decades. It is worth mentioning that alloy-based anodes with a hybrid cathode have been commercialized by Sony in a Nexelion configuration. Unlike that of the insertion process, an alloy and conversion-type electrode experiences several issues that need to be addressed, such as large volume variation, capacity fading upon cycling, and a significant irreversible capacity loss (ICL) during the first cycle,[15] before being employed as prospective an anode in cells for practical configurations.

Although insertion materials experience ICL, it is negligible, whereas only 40 to 70% of the initial capacity is found irreversible in alloy and conversion type materials. The ICL may vary from material to material, and morphology to morphology primarily because of the decomposition of the electrolyte solution, which includes solvents and a salt reduction process.[16] Nevertheless, volume variation and capacity fading can certainly be improved by adopting a surface modification process preferably with carbon coating, making a composite with carbonaceous materials, or by preparing the electrode with either an active or inactive matrix.[17] Therefore, eliminating the ICL is critical before the full-cell assembly when using such high capacity conversion or alloy type anodes.[2,18,19] It is clear that the SEI layer is the main culprit for the significant ICL observed in the first cycle, since the Li consumption takes place in an

Dr. V. Aravindan, Prof. S. Madhavi
Energy Research Institute @ NTU (ERI@N)
Nanyang Technological University
Singapore 637553, Singapore
E-mail: aravind_van@yahoo.com; Madhavi@ntu.edu.sg
Prof. Y.-S. Lee
Faculty of Applied Chemical Engineering
Chonnam National University
Gwang-ju 500–757, Republic of Korea
Prof. S. Madhavi
School of Materials Science and Engineering
Nanyang Technological University
Singapore 639798, Singapore
The ORCID identification number(s) for the author(s) of this article can be found under http://dx.doi.org/10.1002/aenm.201602607.

DOI: 10.1002/aenm.201602607

irreversible manner. In this regard, we would like to explore the possible scenarios to mitigate the ICL issues and discuss in detail the fabrication of practical Li-ion cells, i.e., full-cells.

2. Origins of Irreversible Capacity Loss

It is well known that electrolyte solutions are thermodynamically unstable at lower potentials vs Li^+/Li for a negatively polarized surface. The onset potential for the electrolyte decomposition may vary and ranges often reported from ≈0.8 to 2 V vs Li.[20–22] Hence, electrolyte decomposition occurs in an irreversible manner, eventually leading to the formation of a thick layer formed over the surface. The thickness of the SEI layer may vary from a few angstrom (Å) to tens or hundreds of Å (**Figure 1**). Further, it is very difficult to estimate the exact thickness of the SEI layer since some of the by-products are soluble in an electrolyte solution that is being cycled. Nevertheless, the average thickness of the layer can be estimated using electrochemical impedance spectroscopy (EIS). Generally, an electrolyte solution contains the mixture of cyclic (EC, PC, etc.,) and linear carbonates (DMC, DEC, etc.,) and solvated Li-salt ($LiPF_6$, $LiBF_4$, $LiClO_4$, etc.).

Upon reduction process, there is a competition between the decomposition of the solvated ions and solvent molecules which form inorganic (e.g., Li_2CO_3, LiF, Li_xPF_y, Li_2O, etc.,) and organic (e.g., $(CH_2OCO_2Li)_2$, polyethylene oxide, polycarbonates, etc.,) by-products over the surface of an active material. Interestingly, the inorganic layer forms over the active material and a porous organic layer is formed over the inorganic layer while using carbonaceous anodes. More clearly, the inorganic layer forms towards the electrode side while the organic layer can be found adjacent to the electrolyte side. The SEI formation will continue upon the cycling process, but the predominant Li-consumption is noted in the first cycle only. Further, the composition of the SEI layer is different for different materials, for example, graphite and alloy type anodes (Si and Sn based anodes) have entirely different compositions. The SEI layer is necessary for the safe operation of the cell, especially for graphite. This certainly prevents the solvent molecule

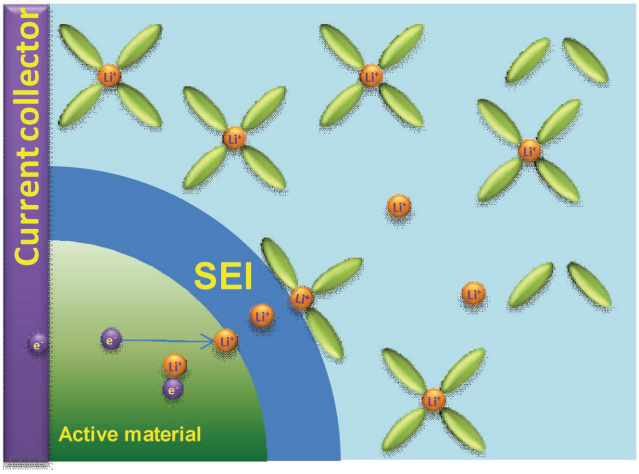

Figure 1. Schematic representation of the SEI formation.

Vanchiappan Aravindan is currently working as a Senior Scientist at the Energy Research Institute @ NTU (ERI@N), Nanyang Technological University, Singapore. He received his Ph.D in 2009 from Gandhigram Rural University, Gandhigram, India. Then, he joined Chonnam National University, Gwang-ju in Korea as a Postdoctoral Fellow with Prof. Yun-Sung Lee. In 2010, he moved to this organization to continue his research career. His research interest includes the development of high performance electrodes and electrolytes for Li-ion chemistry and beyond.

Yun-Sung Lee is currently working as a Full Professor at Chonnam National University, Gwang-ju, Korea. He received his M.S from Chonbuk National University in 1998 and his research work was carried out under the guidance of Prof. Kee-Suk Nahm. He received his Ph.D in 2001 in Applied Chemistry from Saga University in Japan under the direction of Prof. Masaki Yoshio. In 2001, he joined Kanagawa University in Japan as a Postdoctoral Fellow and Doctoral Researcher with Professor Yuichi Sato. He joined Chonnam National University in 2003 as an Assistant Professor. His research interests are in the fields of Li-ion batteries, electrode materials, and hybrid capacitor systems.

Srinivasan Madhavi is currently a Professor and Associate Chair (Academic) at the School of Materials Science and Engineering, Nanyang Technological University (NTU), Singapore. She graduated from the Indian Institute of Technology (IIT), Chennai, India, and received her Ph.D from the National University of Singapore. Her research interests include enhancing the performance of energy storage devices such as lithium ion batteries, supercapacitors, and advanced batteries, with the help of multifunctional nanoscale materials as a means of powering printed electronics, to store energy from renewable sources, and for powering electric vehicles. Her focus has been on the fabrication and investigation of nanoscale materials/architectures for electrochemical energy storage devices.

co-intercalation and subsequent exfoliation. It is worth mentioning that LiC_6 is a strong reducing agent.[23] The detailed discussion regarding the SEI formation of the anode and cathodes are described in reviews by Xu,[16,24] Cheng et al.,[25] and Novak et al.[26] Therefore, we briefly discuss the origin of SEI and its influence towards the electrochemical activity.

3. Physical Blending

Physical blending is a simple approach to overcome the ICL issue. Kulova and Skundin[27] studied the pre-lithiation process by simply maintaining the metallic Li over graphite. From the studies, it is clear that the formation of good (i.e., exhibits good ionic conductivity) or bad surface films are completely dependent on the mass loading of both the graphite and metallic Li. A similar strategy, i.e., rolling-on of metallic Li over an amorphous Si surface has been applied to eliminate ICL on alloy type anodes.[28–30] Dimov et al.[31] placed a long, narrow metallic Li strip over the composite Si anode and paired it with a $LiAl_xMn_{2-x}O_4$ cathode. This approach not only overcomes the ICL issues, but also facilitates enhanced cycling of a full-cell. It is worth mentioning that an increase in the metallic Li strip loading leads to the minimum fade upon cycling. Similarly, this approach has been extended to hard carbon to overcome the ICL and is subsequently paired with $LiCoO_2$.[32] The full-cell fabricated with hard carbon alone delivered a coulombic efficiency of only ≈52% in the first cycle. However, the efficiency was increased dramatically to ≈86% when the metallic Li is pressed tightly over the surface of the hard carbon.

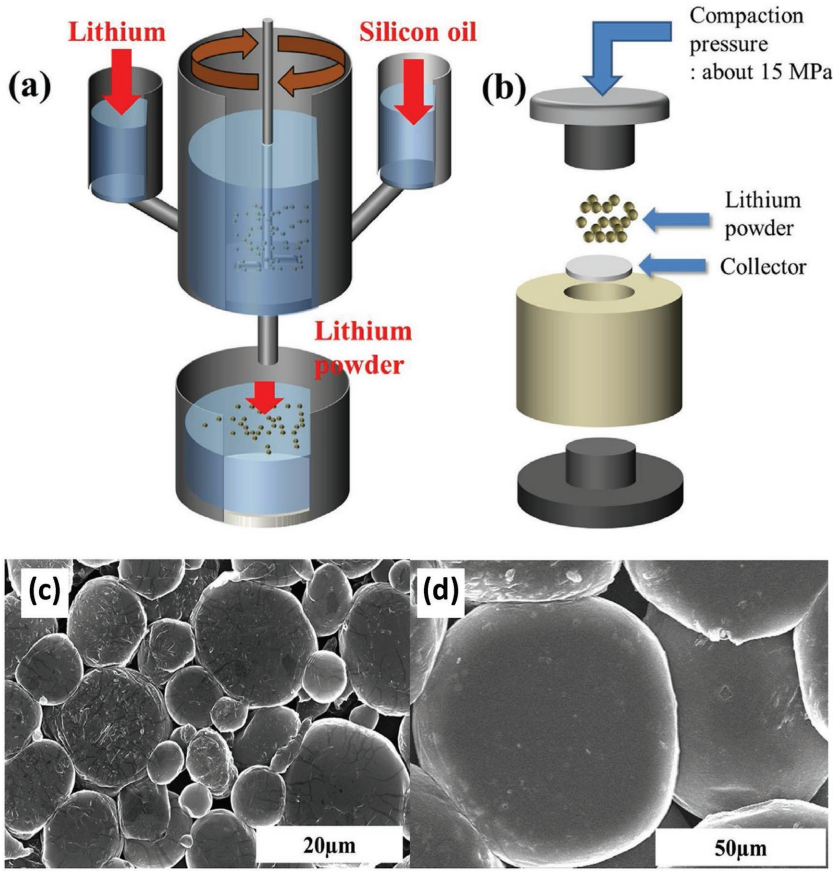

Figure 2. a) Schematic of the DET. b) Schematic of pressing apparatus used for producing Li powder electrode, Li powder electrode (LPE) prepared from Li particles of average size of c) 15 μm and d) 55 μm. Reproduced with permission.[37] Copyright 2014, Elsevier.

4. Li-Metal Powder

Instead of using the metallic strips, the usage of power provides beneficial effects owing to the extended contact with a high specific surface area, homogeneous distribution, and a significantly lower amount of Li is required. Therefore, efforts are attempted to synthesize the Li metal powder and stabilize the surface to prevent the undesirable side reactions.

The droplet emulsion technique (DET) is an important and efficient approach to stabilize the metallic Li powder.[33–37] The DET process yields a formation of a homogeneous protective layer over the Li powder, which is comprised of Li_2CO_3 and LiF.[38] Park and Yoon[33] evaluated the electrochemical performance of DET stabilized Li powder and foil with a MnO_2 cathode in the primary cells. Due to the higher BET surface area, the Li powder delivers a longer discharge time with less of an increase in the resistance regarding the storage period compared to foil. Seong et al.[39] noted the remarkable enhancement in the coulombic efficiency of the Si anodes in half-cell assembly. Although interesting results are noted for the DET stabilized Li powder, there are no extensive studies that have been published regarding the compensation of ICL in practical LIBs i.e., with commercial cathodes (**Figure 2**).

SLMP is a commercial product from the FMC corporation and is kind of core-shell type particulate. This Li is particulate composed of ≈97% metallic content and the remaining ≈3% corresponds to the Li_2CO_3 layer (**Figure 3**).[40] This Li_2CO_3 concentration acts as protective layer and homogeneously covers the Li particulate and also stabilizes them from the undesirable side reactions.[41] As a consequence, handling in dry room conditions is possible rather than a conventional glove box environment. The SLMP can deliver a capacity of ≈3600 mA h g^{-1}, which can alleviate the ICL issues for high capacity negative electrodes (e.g., alloying and conversion), non-lithiated cathodes (e.g., V_2O_5), and conventional carbonaceous materials (e.g., hard carbon).[42]

The SLMP is exposed to a solvent such as *N*-methyl-2-pyrrolidone (H_2O content: 6000 ppm) and exhibits excellent stability for a longer period of time irrespective of temperature (25 or 55 °C), which is certainly useful for the safe operation of the cell during elevated conditions.[43] Utilizing SLMP is one of the efficient approaches to overcome the ICL issue. This technique can be used for the fabrication of LIB with high capacity

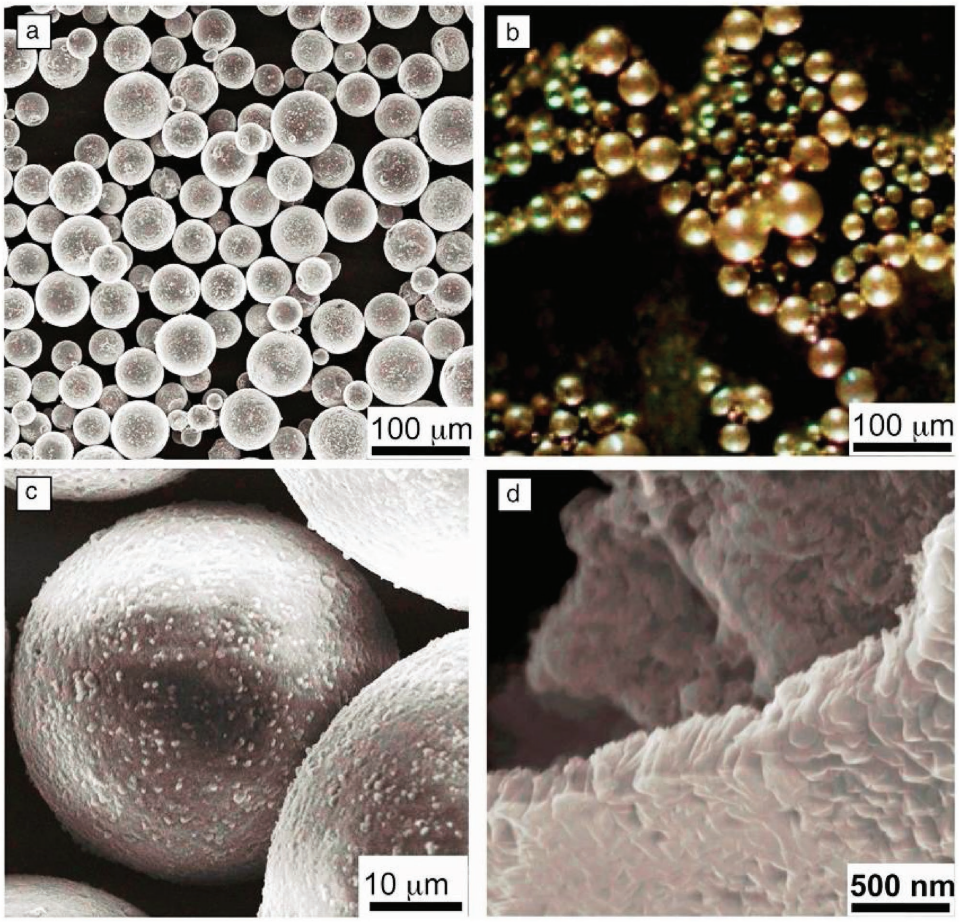

Figure 3. a) Low magnification scanning electron microscopy (SEM) image of stabilized lithium-metal powder (SLMP) particles. b) Optical microscopic image of SLMP particles. Image courtesy of FMC Lithium Corporation. c) High magnification SEM image of the SLMP. d) High magnification SEM image of the lithium carbonate coating layer. Reproduced with permission.[41] Copyright 2014, Cambridge University Press.

materials: (i) to overcome the ICL issue via the formation of the SEI layer in the first cycle, and (ii) pave the way for the possible exploitation of non-lithiated, high capacity cathodes such as V_6O_{13} and V_2O_5 rather than simply using the small capacity cathodes such as $LiCoO_2$, $LiFePO_4$ and $LiMn_2O_4$. Further, this technique can directly be used along with the conventional cathodes by calculating the ICL estimated from half-cell studies with manifold advantages such as (i) the concentration can be tailored based on the requirements, (ii) uniformly distributed over the surface of the electrode, (iii) possibility of material handling in dry atmospheric conditions, (iv) the immediate reaction observed when the electrolyte is introduced and eventually forms the SEI layer, and (v) there is no residual Li left after the SEI formation. Jervis et al.[44,45] reported the possibility of using this concept to overcome the ICL observed from the graphite anode while pairing with cathodes such as LiV_3O_8, $LiCoO_2$, and V_6O_{13}. A notable increase in the coulombic efficiency and cyclability is observed for the case of the $LiCoO_2$/graphite system. Li and Fitch[42] compared the performance of spinel $LiMn_2O_4$ with both graphite and hard carbon electrodes (**Figure 4**). An ≈50% increase in the coulombic efficiency is noted with respect to the baseline capacity for the hard carbon based system. On the other hand, apart from the enhancement in coulombic efficiency, an excellent capacity retention characteristics is also noted for the SLMP added graphitic anode.

In addition to the usage in lower potential anodes, the SLMP has been used to avoid the small ICL observed from the transition-metal-oxide-based insertion anodes. Anatase TiO_2 is a perfect example for this category. Additionally, it is well-known that the anatase phase experiences a significant irreversibility compared to the other metal-oxide-based insertion hosts.[7] Therefore, the same strategy has been applied to mitigate the issue, i.e., spray over the surface of the TiO_2 electrode and pair with a ZnO modified $LiNi_{0.5}Mn_{1.5}O_4$ cathode. As expected, this process exhibits substantial improvement in the cyclability.[46] Apart from the advantages mentioned above, a small reduction in the reversible capacity is also noted compared to the bare system. Similarly, a notable increase in the coulombic efficiency is observed for α-Fe_2O_3@graphitic carbon microsphere systems in a half-cell assembly.[47]

Forney et al.[48] introduced the concept of pressure activation of the SLMP sprayed over a Si-CNT composite and subsequently paired with a $Li(NiCoAl)O_2$ cathode. As a consequence, an enhancement in the reversible capacity and cyclability is noted when compared to an unpressurized system. Interestingly, no prominent region appears for the SEI formation in the

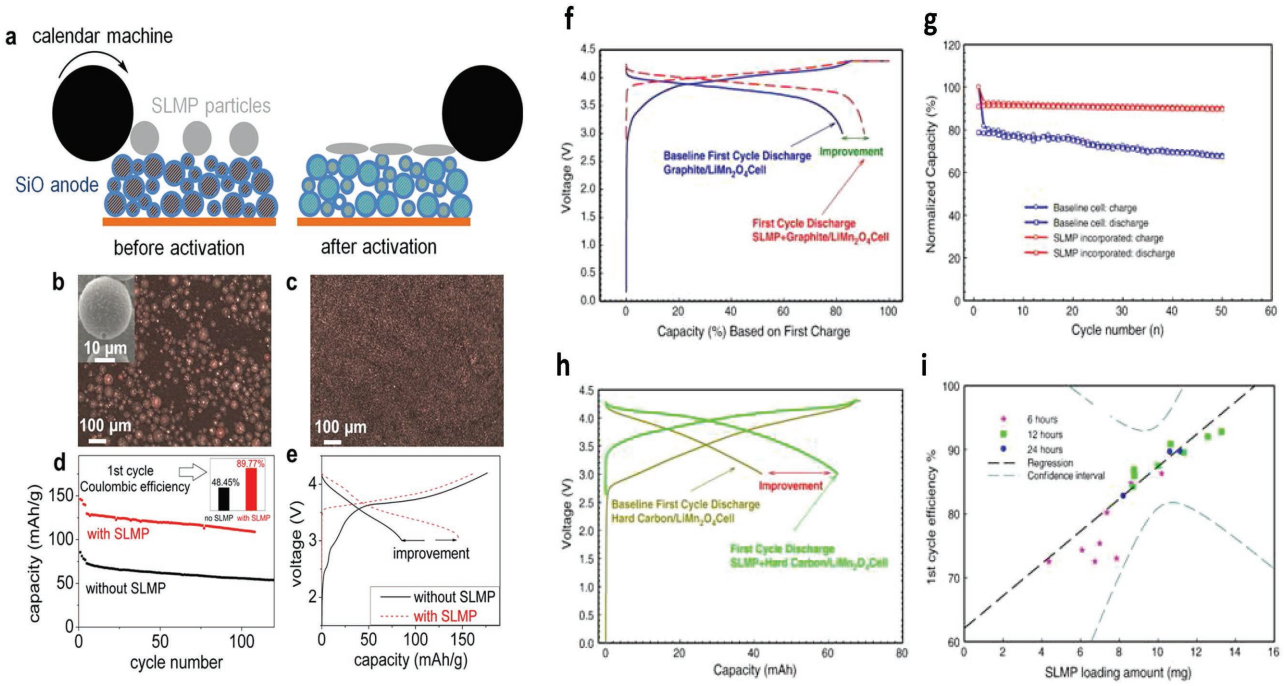

Figure 4. a) Schematics of the utilization of SLMP for the SiO electrode. SLMP particles are loaded on to the SiO anode. Rolling compression was used to crush the Li_2CO_3 shell of SLMP to release lithium metal and laminate it on the surface of SiO electrode. This process is called SLMP activation. b) SLMP particles loaded on the SiO electrode before activation. The inset shows the SEM image of a single SLMP particle. c) SiO electrode surface after electrolytes are added onto the SiO electrode with activated SLMP after 12 h. This shows the disappearance of SLMP and indicates the successful pre-lithiation of the SiO electrode. d) SiO/NMC full cell performance with or without the SLMP capacity-enhancement additive, two cycles at C/20, two cycles at C/10, and then C/3. Reproduced with permission.[49] Copyright 2014, American Chemical Society. e) First cycle voltage curves of the two cells, Examples of full cell performance enhanced by SLMP f) the 1st cycle efficiency improvement for graphite/$LiMn_2O_4$ cells; g) the cycle performance improvement for graphite/$LiMn_2O_4$ cells. h) the increased delivered capacity in 1st cycle for hard carbon/$LiMn_2O_4$ cells. i) the effects of SLMP loading amount and pre-condition time on the 1st cycle efficiency improvement for hard carbon/$LiMn_2O_4$ cells. Reproduced with permission.[42] Copyright 2011, Elsevier.

aforesaid assembly during the first charge when compared to the non-activated SLMP and the SLMP free system. The activation process is simply a breakdown of protective layer where Li_2CO_3 appears over the metallic Li particulates through the use of a normal stainless steel rod. Zhao et al.[49] adopted a similar SLMP activation process for the SiO anode by running a calendar machine optimized at 5% with a functionalized conductive polymer binder poly (9,9-dioctylfluorene-*co*-fluorenone-*co*-methylbenzoic ester). As a result, a dramatic increase in the coulombic efficiency from ≈48 to ≈90% is observed and paired with $LiNi_{1/3}Mn_{1/3}Co_{1/3}O_2$ (NMC) cathode, apart from the enhancement of high reversible capacity (**Figure 5**). Similarly, an excellent cycling stability and effective utilization of SLMP is reported for an amorphous hierarchical GeO_x nanostructure when paired with NMC.[50] Wang et al.[51] also observed a similar type of improvement in the NMC cathode when paired with a graphite anode in the presence of SLMP.

Yersak et al.[52] first reported the fabrication of Li-free material as an electrode, for example FeS+S composite that has been used as cathode, and Si-Ti-Ni ($Ti_4Ni_4Si_7$) alloy is explored as composite anode in the presence of 77.5 Li_2S:22.5 P_2S_5 glass ceramic. SLMP has been effectively used to overcome the ICL and supply the necessary Li during electrochemical cycling ($Li_{3.2}Ti_4Ni_4Si_7$). Good cyclability is noted for the mentioned configuration, which clearly suggests that SLMP could be effectively used in both liquid and solid-state configurations. The influence of a styrene butadiene rubber–PVDF composite binder on the electrochemical properties with SLMP has been reported with graphite anode.[53] This new composite binder system certainly improves the mechanical properties without compromising the ionic conductive properties of the PVDF binder. As a result, there is negligible ICL in the first cycle and good cyclability is noted for the new binder system compared to the conventional PVDF. Most of the studies are conducted in the reductive atmosphere of electrolyte solutions, i.e., anode materials, but an oxidative atmosphere is also reported. For example, Hu et al.[54] studied the enhanced electrochemical activity of a $LiNi_{0.5}Mn_{1.5}O_4$ cathode with metallic Li and graphitic anodes. Apart from LIBs, the SLMP have a bright future with the other Li-ion chemistries such as a Li-S system, when using non-metallic compounds especially Li_2S. Since Li_2S is thermodynamically unstable in air because of its moisture, carbonaceous materials are blended to minimize the direct contact with atmosphere. In such cases, activation of Li_2S is desperately required for stable operation of the cell. Zheng et al.[55] succeeded in the attempt by exploiting the SLMP to overcome the ICL by spraying the particles on the microporous carbon composite. An exceptional cyclability with a high reversible capacity is noted. In addition to the use in Li-based batteries, SLMP is also effectively used in the Li-ion capacitor industry for the pre-lithiation of carbonaceous insertion hosts such as hard carbon and graphite. Nam et al.[56] suggest the possibility of constructing symmetric pseudo-capacitors using non-lithiated metal oxides in the presence of an organic

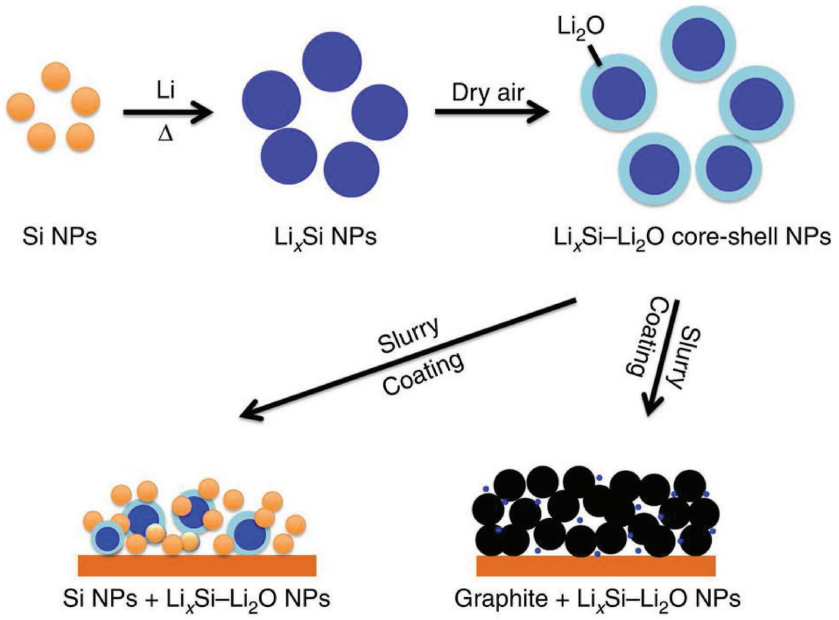

Figure 5. A dense passivation layer is formed on the Li_xSi NPs after exposure to trace amounts of oxygen, preventing the Li_xSi alloy from further oxidation in dry air. As-synthesized $Li_xSi–Li_2O$ core–shell NPs, compatible with the existing battery-manufacturing environment, can be mixed with various anode materials during slurry processing and serve as an excellent pre-lithiation reagent. Reproduced with permission.[60] Copyright 2014, Nature Publishing Group.

electrolyte to widen the energy density. To circumvent the capacity loss in the first cycle, SLMP has been employed successfully. Interestingly, increasing the SLMP loading in hard carbon results in the decrease in the open circuit potential, which plays a crucial role in determining the cyclability of a Li-ion capacitor.[57–59]

Interestingly, Zhao et al.[60,61] reported the thermal alloying process for the preparation of Li_xSi-Li_2O core shell nanoparticles. This has been prepared by melting metallic Li at 200 °C and the inclusion of the stoichiometric amount of Si ($Li_{4.4}Si$), and then stirred for 6 h within a glove box environment. The trace amount of moisture present in the glove box triggers the Li_2O surface layer (≈10 nm) formation. This simple process not only overcomes the ICL issue in Si, but also can be used along with any one of the high capacity anodes, including graphite. As mentioned above, the inclusion of the Li_xSi-Li_2O core shell nanoparticles leads to the drop in cell potential. Further, the Li_xSi-Li_2O core shell nanoparticles are highly stable in humid conditions (i.e., –30 °C, –50 °C) compared to a dry or normal atmosphere. However, longtime exposure to the aforementioned medium leads to the growth of a thick Li_2O layer (approximately 10 to 20 nm thick, Figure 5).

5. Sacrificial Salts

The excellent advantage of using SLMP is the ability to overcome the ICL issues for negative electrodes. However, the SLMP have several issues: (i) spraying over active particulates leads to the dilution of volumetric capacity; (ii) incorporation of metallic Li to either electrode poises the potential at 0 V, thereby triggering various unwanted side reactions; and (iii) a question regarding the possibility of fabricating LIBs in air atmosphere (at least dry room required). Armand et al.,[62] reported the possibility of using Li-salt with oxidizable anions during the formulation of the positive electrodes (**Figure 6**). Upon first charge, the anions lose their electrons which are eventually converted into innocuous gaseous products such as

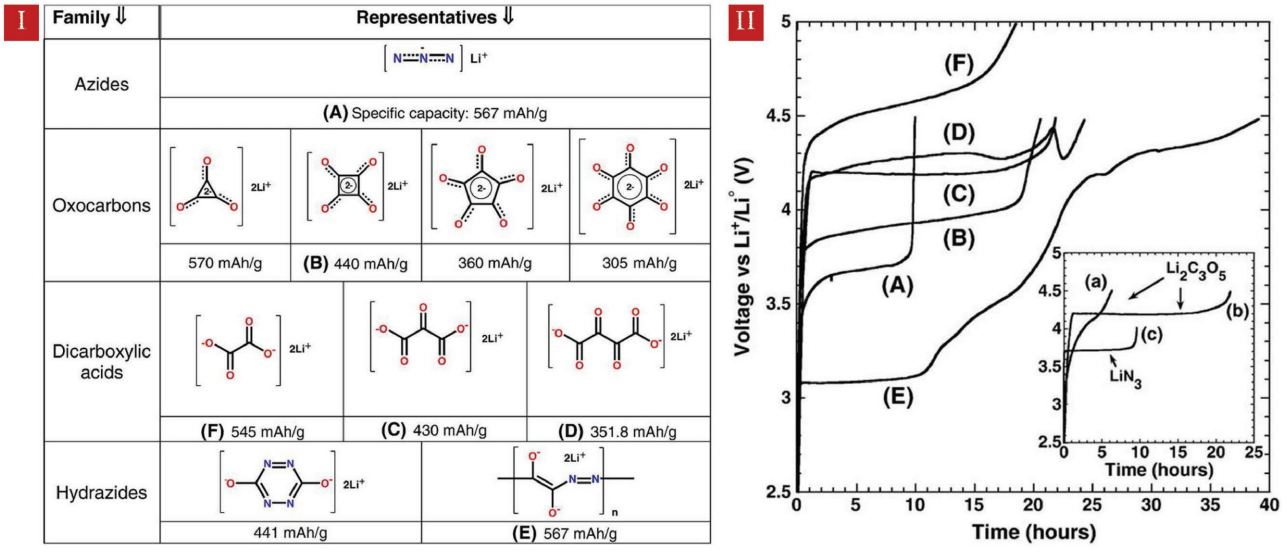

Figure 6. I) Structural formula and specific capacity of the compounds corresponding to the four "sacrificial salt" families, and II) Charge curves of A) LiN_3, B) $Li_2C_4O_4$, C) $Li_2C_3O_5$, D) $Li_2C_4O_6$, E) $[COCON(Li)N(Li)]_n$, and F) $Li_2C_2O_4$ mixed with 30% Ketjen black carbon (KJ-600); rate 1 Li^+ in 10 h; inset: comparison of the effect of SP and KJ-600 carbons where a) $Li_2C_3O_5$ + 30% SP-C (ball milled), b) $Li_2C_3O_5$ + 30% KJ-600, and c) LiN_3 + 30% SP-C. Reproduced with permission.[62] Copyright 2010, Elsevier.

N_2, CO, and CO_2 within the potential working range of 3–4 V vs Li. The working potential range is more suited for conventional cathodes such as $LiCoO_2$, $LiMn_2O_4$, and $LiFePO_4$. In addition, the evolution of such gaseous products generates porosity in the composite electrode, thereby facilitating faster Li-ion kinetics. The gases could be evacuated before sealing the battery, or through a safety vent. On the other hand, several Li-ion cells are charged without the lid (bag) sealed to avoid pressure ($H_2C = CH_2$) build-up. Here, the authors reported azide (LiN_3), squarate ($Li_2C_4O_4$), oxalate ($Li_2C_2O_4$), ketomalonate ($Li_2C_3O_5$), and di-ketosuccinate ($Li_2C_4O_6$) as possible sacrificial salts for the compensation. In situ studies clearly revealed the evolution of the gases due to the charging process while using sacrificial; salts previously discussed. The LiN_3 salt would be simplest and most commercially available for the use in all range of cathodes like $LiCoO_2$, $LiMn_2O_4$, and $LiFePO_4$ when compared to the other salt compounds. This salt will decompose according to the following reaction, $2LiN_3 \rightarrow 2Li^+ + 2e^- + 3N_2\uparrow$. Although it is interesting to see the advantages of the sacrificial salts, the drawbacks are certainly worth mentioning. For example, azides are toxic and commercially not available, but the decomposition potential of the oxalates are found beyond the thermodynamic stability of electrolyte solution. Unfortunately, no battery performances with high ICL anodes are reported when using these types of salts.

6. $Li_{2.6}Co_{0.4}N/Li_3N$ Decomposition

Li_3N is one of the most highly ionic conducting materials intended for solid electrolytes and exhibits the conductivity in mS cm^{-1}. The ionic migration is parallel to the Li_2N^- direction along with its layered arrangements.[63] Unfortunately, the decomposition potential (≈0.5 V vs Li) is the main challenge to employ the material as a negative electrode in secondary batteries. It has been reported that Li_3N could be used as a reservoir for the compensation of the ICL observed from the high capacity conversion and alloy type anodes, for example, Si-Li_3N composite.[64] Yersak et al.[65] used Li_3N as a source for Li with regards to the fabrication of all solid-state batteries based on the following electrolytic ratio $80Li_2S{:}20P_2S_5$, in which indium metal is utilized as the negative electrode and Li_3N/TiS_2 composite as the positive terminal. Influence of the Li:Ti ratio has been investigated and found that a ratio of 3:1 is appealing in terms of high reversibility and cyclability. Amatucci et al.[66] reported the mechanically assisted reduction of Li_3N for the prelithiation of high capacity metal fluorides. Recently, Park et al.[67] attempted to explore the possibility of using Li_3N as a cathode additive to improve the coulombic efficiency while pairing with Si nanoparticles covered with SiO_x and carbon layer, as an anode. Blending the Li_3N with $LiCoO_2$ improves the reversible capacity, but the coulombic efficiency and rate performance are severely affected irrespective of the concentration. Therefore, a modification in the strategy is required. Accordingly, the Li_3N layer was deposited over the surface rather than blending, which certainly improves the electrochemical activity.

Rather than using bare Li_3N, the transition metal doped Li_3N structure based on $Li_{3-x}M_xN$, M = Co, Ni, Cu, Mn and Fe[63] is also explored. From the possible options, $Li_{2.6}Co_{0.4}N$ exhibits impressive results by delivering a specific capacity of over 700 mA h g^{-1}.[68–79] It has become the popular material for the compensation of ICL for variety of negative electrodes; for example natural graphite,[80] MCMB,[81,82] hard-carbon,[83] Si-graphite composite,[84] $SnSb_x$,[85–92] SnO,[89,93,94] SiO_x,[93,95] $LiTi_2O_4$,[96] TiP_2O_7[97] and Co_3O_4 ($Li_{2.6}Co_{0.2}Cu_{0.2}N$).[90] Also, the potential use of $Li_{3-x}M_xN$ in regards to the fabrication of all solid-state batteries has been highlighted by Takeda et al.[98] in the review (**Figure 7**).

7. Artificial SEI

Artificial SEI formation is another interesting approach exploited for circumventing the ICL issue. The reduction of solvent molecules leads to the formation of SEI layer, naturally. However, artificial SEI has been formed via the electrolyte additives, or usage of a binder, however, electrolyte decomposition cannot be avoided. Nevertheless, the usage of additives certainly leads to the suppression of a significant ICL via facilitating the SEI formation over the active material. This concept has been

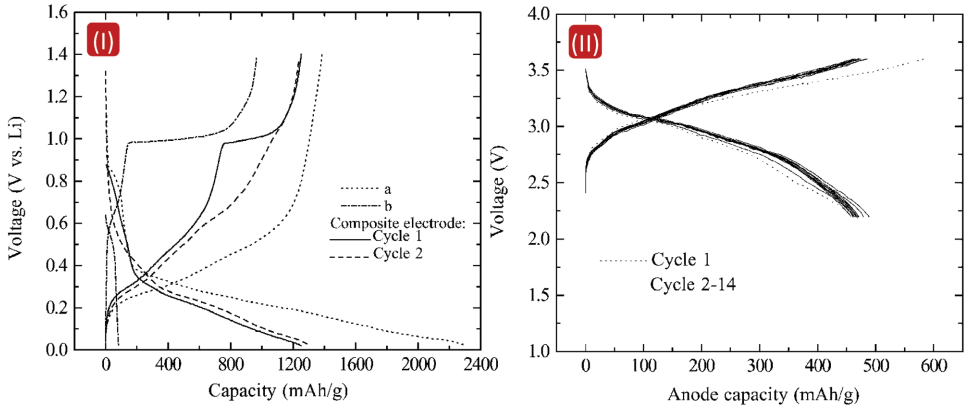

Figure 7. I) The initial cycle profiles for SiO, $Li_{2.6}Co_{0.4}N$, and their composite. (a) 20% AB, 11% PVDF, 4% PTFE and 65% SiO; (b) 8% AB, 4% PVDF, 2% PTFE and 86% $Li_{2.6}Co_{0.4}N$. Composite electrode: 21% AB, 11% PVDF, 4% PTFE, 32% $Li_{2.6}Co_{0.4}N$ and 32% SiO. $i_c = i_d = 0.2$ mA cm^{-2}, and (II) The charge and discharge profile for a cell with $SnSb_{0.14}$/ $Li_{2.6}Co_{0.4}N$ composite anode and $LiCo_{0.2}Ni_{0.8}O_2$ cathode. $i_c = i_d = 0.4$ mA cm^{-2}. Reproduced with permission.[91] Copyright 2002, Elsevier.

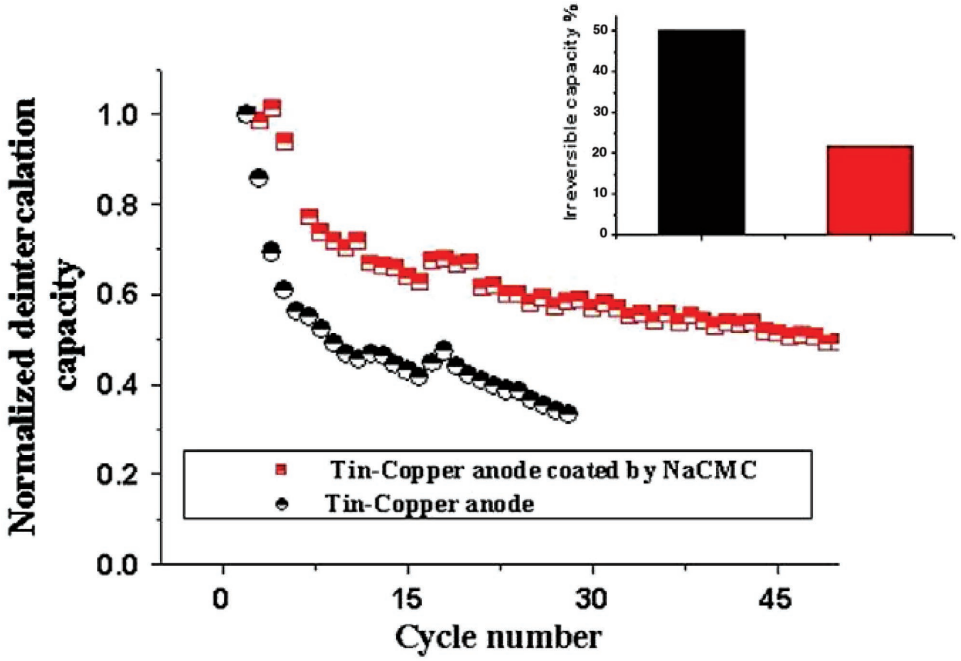

Figure 8. Normalized de-intercalation capacity as a function of cycle numbers of the ART-SEI modified and pristine tin–copper anodes. Reproduced with permission.[99] Copyright 2009, Elsevier.

predominantly used for graphitic anodes with an additive concentration of less than 5%. Numerous electrolyte additives have been used for this purpose which has been described by Zhang[100] in his critical review. Later, Menkin et al.[99] effectively used the Na-CMC binder for the development of an artificial SEI formation to suppress the ICL of Sn-Cu alloy anode by 20–50% (**Figure 8**). Here, the Na-CMC has been chosen because of the thermal stability and self-heating ability when undergoing a large volume variation upon the charge–discharge processes. Furthermore, CMC forms a 3D cross-linked network via intra-and intermolecular hydrogen bonding between the carboxyl and hydroxyl groups in an acidic environment. Unfortunately, there are no full-cell studies reported using this approach. However, the Li metal has been protected by Li_3PO_4 deposition, which eventually acts as an interface layer and leads to the development of Li-metal batteries with a $LiFePO_4$ cathode.[101] However, few reports are available on the usage of such an artificial layer to protect Li_xSi anode[102] and graphite.[103]

8. Chemical Lithiation

Chemical lithiation is one of the well-established procedures for lithiation, especially for insertion type electrodes. Generally, *n*-butyl Li in hexane or LiI in acetonitrile will be used for this process.[104–107] Recently, Li_2S has also been used to fabricate Li-ion-S systems.[108] Johnson et al.,[109] reported better electrochemical activity for the lithiated MnO_2 phase in terms of better cyclability and capacity retention characteristics when compared to its native compound. The pre-lithiation was performed by three procedures (such as *n*-butyl Li, LiI, or direct reaction of α-MnO_2 with $LiOH.H_2O$) and compared. Chemically lithiated phases delivered good cyclability in a half-cell assembly compared to the native phase, however, a small drop in the initial reversibility has to be sacrificed. MoO_2[110,111] and $FeSe_2$[112] are the best examples for this kind. Many of the studies have been conducted for the lithiation of high capacity V_2O_5 electrodes,[113,114] which is mainly due to the richness in the oxidation state of V and associated structural changes.[115] In many cases, the pre-lithiated V_2O_5 showed improved electrochemical activity compared to the bare V_2O_5.[106] Further, many transition metal oxides and chalcogenides have been chemically lithiated using this approach,[116] which are not originally indented for battery point of view, but studied to understand the structural prospects.

Scott et al.[117] reported the complete elimination of ICL for carbon electrodes while treating with *n*-butyl Li in hexane for a longer duration. Such a longer duration lithiation process enables the formation of a very stable SEI layer on carbonaceous electrodes eventually leading to zero loss capacity in subsequent cycling. Cheah et al.[106] chemically lithiated the V_2O_5 phase using *n*-butyl Li in hexane and studied the limited Li-insertion of a mole ($Li_xV_2O_5$, $0 < x < 1$) in both a half-cell and full-cell assembly with $Li_4Ti_5O_{12}$. Unfortunately, the electrochemical performance of the chemically lithiated V_2O_5 is inferior to electrochemically lithiated phase under the same configuration (**Figure 9**). [118]

9. Self-Discharge/Spontaneous Lithiation Mechanism

Liu et al.[119] proposed a simple pre-lithiation procedure to overcome the ICL issue for high capacity anodes. According to Liu et al.,[119] maintaining the active material in direct contact

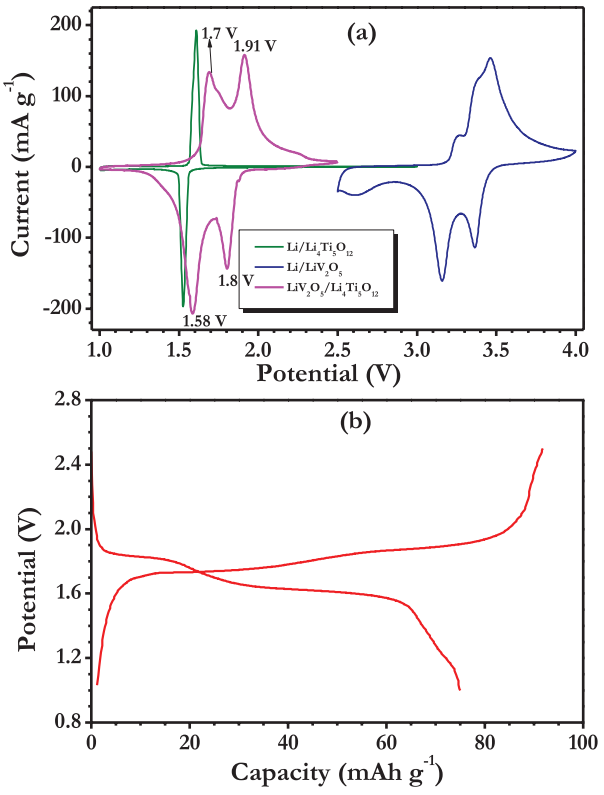

Figure 9. a) Cyclic voltammograms (CV) of chemically lithiated LiV_2O_5/$Li_4Ti_5O_{12}$ full-cell between 1.0–2.5 V at scan rate of 0.1 mV s^{-1} in room temperature. The CV traces of half-cells, Li/LiV_2O_5 and Li/$Li_4Ti_5O_{12}$ also provide a comparison recorded at the same scan rate of 0.1 mV s^{-1}. b) Typical galvanostatic charge–discharge curves at current densities of 10 mA g^{-1} (based on cathode loading) at room temperature.

with metallic Li with small pressure and an electrolyte solution is sufficient to trigger the spontaneous thermodynamic reaction, i.e., self-discharging mechanism (often called surface treatment). For example, 20 minutes of direct contact provides a capacity of ≈2000 mA h g^{-1} for Si. In addition, the self-discharge mechanism did not affect the morphological features of the active material that was utilized. As a result, we can clearly study the influence of the morphological features towards the battery performance. Similar to Si anode, pre-lithiation of the Sn-C was also explored and eventually paired with $Li[Ni_{0.45}Co_{0.1}Mn_{1.45}]O_4$[120] and $Li[Li_{0.2}Ni_{0.4/3}Co_{0.4/3}Mn_{1.6/3}]O_2$[121] cathodes. Pre-treating the graphene/γ-Fe_2O_3 composite anode in the presence of a LiBOB-based electrolyte was carried out and the anode was subsequently paired with $LiFePO_4$.[122] As expected, the pre-treated configuration showed a better performance than the untreated case.

Scrosati et al.[123–134] and Hassoun et al.[131–137] made extensive use of this pre-treating technique for various configurations. For instance, pre-lithiated Si with $Li[Ni_{0.75}Co_{0.1}Mn_{0.15}]O_2$,[123] Sn-C with carbon-coated $LiFePO_4$,[124,125,128] $LiNi_{0.5}Mn_{1.5}O_4$,[126,127,133,135] and $LiFe_{0.1}Co_{0.9}PO_4$[136] were tested. For many of the cases, drastic suppression of the ICL is noted from 63 to 14% by using this technique, although good electrochemical reversibility is noted for graphene nanosheets (GNS). However, there is no promoted electrochemical activity as observed with a $LiFePO_4$ cathode.[138] This is primarily because of the electrolyte decomposition and associated continuous SEI formation upon cycling. However, a GNS based full-cell delivered a reasonably improved cyclability compared to a graphitic anode. The same authors extended the studies for the comparison of electrochemically, pre-lithiated and pre-lithiation via self-discharge mechanism for a GNS anode with a $LiFePO_4$ cathode.[139] The studies clearly indicate a much better performance for the $LiFePO_4$/GNS cell is evident by using the latter procedure (i.e., self-discharge mechanism). These results have been paralleled by Hassoun et al.[140]

In the same manner, graphene-$ZnMn_2O_4$ composite electrode is also pre-lithiated via a self-discharge mechanism to fabricate the full-cell with $LiFePO_4$ cathode.[141] Wang et al.[142] suggested the remarkable improvement in the coulombic efficiency from ≈71 to 98% for an onion-like, carbon/MoS_2 composite in the first cycle after the pre-lithiation process. In a typical process, the electrode was covered with metallic Li, i.e., direct contact with Li in the presence of electrolyte (without any separator) for a conventional CR 2032 configuration for 24 h. MnO is one of the preferred conversion anodes exploited for LIB applications, typically, the surface treated anode, by delivering excellent cyclability of over 300 cycles when coupled with $LiNi_{0.5}Mn_{1.5}O_{4-\delta}$ cathode.[143]

Sun et al.[144–146] compared the electrochemical performance of pre-treated porous carbon-Fe_3O_4, composite with an electrochemical route. Interestingly, both cells exhibit better cyclability when paired with $LiNi_{0.59}Co_{0.16}Mn_{0.25}O_2$ cathode for 1000 cycles. Furthermore, the same group of authors[144,146] reported the performance of Fe_3O_4-FeF_2 and Fe_3O_4@CF_x composite anodes with $LiNi_{0.5}Mn_{1.5}O_4$ by adopting similar pre-treatment procedures. Additionally, this approach has been extended to the fabrication of Li-ion-S batteries via a self-discharge mechanism by using different anodes such as Li_xSi,[147] pre-lithiated Si–SiO_x with S,[129] an electrodeposited Si–O–C anode and paired with Li_2S-MCMB,[131] a Sn–C anode with S–C composite,[137] and pre-lithiated graphite.[134] Additionally, the approach was extended to the Li-ion-O_2 system as well, in which the Si anode was activated (Li_xSi) using the self-discharge mechanism.[132]

10. Electrochemical Lithiation

Electrochemical lithiation is one of the simplest processes to be used in lab scale and industry, irrespective of anode or cathode. Initially, electrochemical lithiation was used for both electrodes in order to stabilize them via SEI formation with metallic Li. For example, a $LiMn_2O_4$/disordered carbon system where both electrodes were separately tested with Li for five cycles and then paired.[148] This process certainly overcomes the ICL observed in both electrodes. In the same way, Caballero et al.[149] extended the pre-lithiation process for the Cherry and Olive stone derived carbons when coupled with $LiMn_2O_4$ cathode. Similarly, for the case of the $LiFePO_4$/Fe_2O_3 configuration, the $LiFePO_4$ cathode was charged to 4 V vs Li (to extract the Li to form Li_0FePO_4) and Fe_2O_3 was discharged to 0.3 V vs Li to allow for the conversion reaction to take place ($2Fe^0 + 3Li_2O$).[150] Then, both electrodes will have been coupled for the completion of the cell fabrication. Later, this two-electrode treatment is also

used for the fabrication of $LiNi_{0.5}Mn_{1.5}O_4$/Sn-C cell, in detail, $LiNi_{0.5}Mn_{1.5}O_4$ is charged up to 5 V vs Li ($Li_0Ni_{0.5}Mn_{1.5}O_4$), whereas Sn-C has been cycled for about 20 cycles in a half-cell assembly and finally discharged to 0.01 V vs Li before conducting full-cell assembly.[151] ICL, observed for a cathode, is negligible compared to either the conversion or the alloy type anodes under balanced mass loadings; hence, treating both the anode and cathode is a time-consuming process. Therefore, treating the high capacity anode is sufficient. For example, Aurbach et al.[152–154] pre-treated the column for a-Si thin films in a two-electrode coin cell configuration in the presence of FEC, which form the passivation layer. Later, the pre-treated Si film was paired with cathodes such as TiS_2,[154] $LiNi_{0.5}Mn_{1.5}O_4$[153] and S[152] thereby, rendering excellent electrochemical activity. The CuO-MCMB composite is also galvanostatically treated for two cycles in a half-cell assembly and subsequently paired with high voltage cathodes such as $LiNi_{0.5}Mn_{1.5}O_4$[155] and $Li_{0.85}Ni_{0.46}Cu_{0.1}Mn_{1.49}O_4$[156] to eliminate the ICL. Similarly, Fe_2O_3-MCMB[157] and NiO-MCMB[158] composites were also subjected for two cycles in a half-cell assembly, prior to the fabrication of a full-cell using $Li_{1.35}Ni_{0.48}Fe_{0.1}Mn_{1.72}O_4$ and $LiNi_{0.5}Mn_{1.5}O_4$ cathodes, respectively.

Aravindan et al.[159] also reported the fabrication of $LiMn_2O_4$-based assembly with an electrochemically treated Fe_3O_4-graphene composite[159] and red mud as anodes.[160] Chae et al.[161] reported on the excellent cyclability of galvanostatically cycled carbon-coated MnO_x anodes with $LiMn_2O_4$ for over 300 cycles. Scrosati et al.[162] extended the same strategy for pre-treating the various anodes before being paired with cathodes, for instance, mechanically milled Sn-C anode with $LiNi_{0.5}Mn_{1.5}O_4$,[162] Sn-Co-C ternary composite anode with $LiNi_{0.5}Mn_{1.5}O_4$[163] and $LiFePO_4$[164] cathodes. It is well-known that GNS has always displayed high ICL values irrespective of the synthesis procedures employed. In this line, Vargas et al.[165] utilized the electrochemical pre-lithiation process for GNS before being coupled with a high voltage spinel cathode ($LiNi_{0.5}Mn_{1.5}O_4$). All nanowire-based Li-ion cells were reported by Wang et al.[166] using $LiMn_2O_4$ as cathode and Mn_2O_3 as anode.

Different levels of pre-lithiation and its influence on the electrochemical performance of $ZnFe_2O_4$/$LiFePO_4$ have been reported by Varzi et al.[167] In all cases, a highly lithiated phase showed much better performance than non-lithiated and partially lithiated phases in terms of cyclability and capacity perspective for the respective configurations. Jayaraman et al.[168] also suggested the exceptional cyclability of 4000 cycles for pre-treated electrospun α-Fe_2O_3 anode along with a spinel cathode ($LiMn_2O_4$). Apart from the efficient usage of this technique for the conversion and alloy type anodes, Aravindan et al.[118,169,170] reported the fabrication of a rocking-chair-type LIB with pre-lithiated V_2O_5 by restricting the reversible insertion of 1 mol. of Li (LiV_2O_5) and $Li_4Ti_5O_{12}$ anodes to match the electrochemical activity of this configuration similar to $LiFePO_4$ (**Figure 10**). Similarly, the 2.2 V class Li-ion cells were assembled with pre-lithiated graphite (LiC_6) and carbon coated NASICON type $LiTi_2(PO_4)_3$ as the cathode.[169] Likewise, the same concept was extended for the anatase-phase TiO_2, in which the electrospinning procedure was used for the preparation of said metal oxide.[170] On the counter side, the pre-lithiated graphite (LiC_6) was exploited to establish the working potential of ≈1.6 V.

11. Overlithiated Cathodes

The concept of using chemically overlithiated spinels was first proposed by Tarascon et al.[171] in the 1990s for carbon anodes while pairing with spinel cathodes ($LiMn_2O_4$) which was followed by the research from Peramunage and Abraham[172] for the same system. Spinel cathodes such as $LiMn_2O_4$ and $LiNi_{0.5}Mn_{1.5}O_4$ are a special type of materials that exhibit electrochemical activity at ≈4 and ≈4.7 V vs Li, respectively.[8,173–175] The observed potential is due to the utilization of tetrahedral (8a) $Mn^{3+/4+}$ and $Ni^{2+/4+}$ redox couples in the $LiMn_2O_4$ and $LiNi_{0.5}Mn_{1.5}O_4$, respectively. Further, both materials contain empty octahedral sites (16c) for the reversible insertion of one mole of Li with a corresponding theoretical capacity of ≈148 mA h g^{-1} at ≈2.7 V vs Li.[176,177] Unfortunately, the cyclability of such an octahedral region is found to be inferior for both cases because of the Jahn-Teller distortion around the Mn^{3+} region. In addition, Li insertion into the octahedral region leads to the formation of a tetragonal phase ($Li_2Mn_2O_4$ and $Li_2Ni_{0.5}Mn_{1.5}O_4$), which cause ≈13% volume variation.[176]

As a consequence, severe fading is resulted. Apart from the aforesaid issues, the working potential of ≈2.7 V vs Li is too low from a cathode point of view and higher from an anode viewpoint. Hence, there are no significant efforts being carried out for this region. Since the emergence of high capacity conversion and alloy anodes, the octahedral region has become more popular and can be used efficiently as a Li-reservoir for the compensation of ICL when observed in such materials. Tarascon et al.[171,178,179] first reported the Li-reservoir approach ($Li_{1+x}Mn_2O_4$) for the fabrication of metal-free Li-ion cells with either carbonaceous or conversion type anodes. The overlithiated cathode is prepared via chemical reduction by using LiI in acetonitrile. The performance of an overlithiated $Li_{1.3}Mn_2O_4$ cathode is compared with native spinel ($LiMn_2O_4$) when paired with a conversion type CoO anode. This overlithation concept not only mitigates the ICL issue, but also delivers a better reversibility than native spinel ($LiMn_2O_4$) when coupled with CoO. Additionally, better electrochemical activity is noted when compared to a $LiCoO_2$/CoO system under similar circumstances.

Rosenberg et al.[180] adopted the same approach for the fabrication of a full-cell using FeSb-TiC composite anode with 4 ($Li_{1.05}Ni_{0.05}Mn_{1.9}O_4$) and 5 V vs Li ($LiNi_{0.5}Mn_{1.5}O_4$) class spinel cathodes. A microwave-assisted procedure is conducted for the aforesaid cathodes for pre-lithiation (chemical lithiation) with different duration times in the presence of tetraethylene glycol with $LiOH.H_2O$ as a Li source. Apparently, the increase in exposure time leads to the insertion of an additional amount of Li. This clearly suggests that the required amount of Li for the compensation of ICL could be easily tailored. The $LiNi_{0.5}Mn_{1.5}O_4$/FeSb-TiC cell is found to be superior in terms of high reversible capacity and cyclability when compared to its Li-rich 4 V vs Li class counterpart. In addition, less self-discharge (1.4% per day) is also worth mentioning for a $LiNi_{0.5}Mn_{1.5}O_4$/FeSb-TiC system compared to 2.3% per day for a $Li_{1.05}Ni_{0.05}Mn_{1.9}O_4$/FeSb-TiC configuration. Similarly, a graphite-based anode also experiences the same issue (2.3% per day) for a time-dependent storage compared FeSb-TiC anode (1.4% per day) when paired with $LiNi_{0.5}Mn_{1.5}O_4$ cathode.

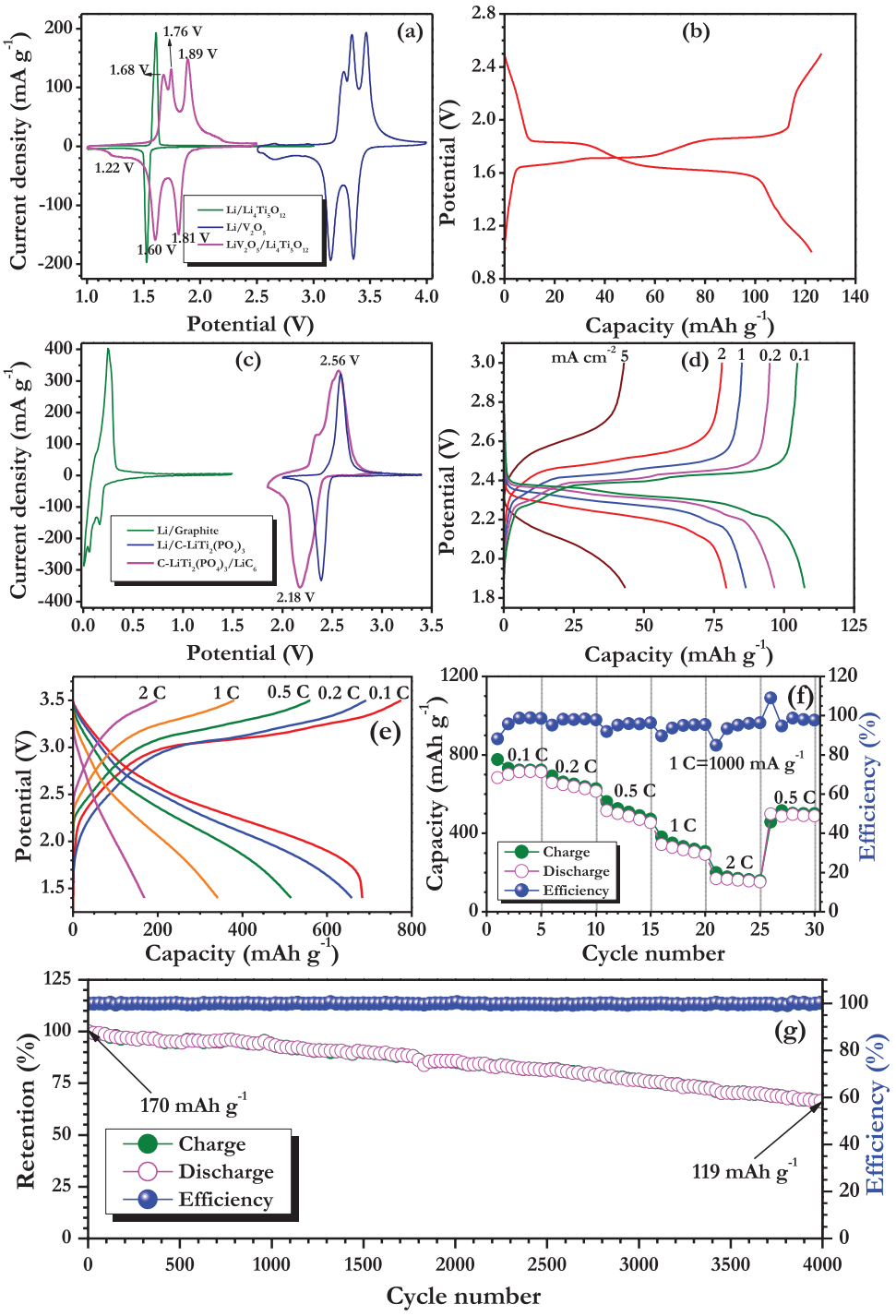

Figure 10. a) CV traces of an electrochemically lithiated $LiV_2O_5/Li_4Ti_5O_{12}$ full-cell between 1.0–2.5 V at a scan rate of 0.1 mV s^{-1} at room temperature. The CV traces of half-cells, Li/V_2O_5 and $Li/Li_4Ti_5O_{12}$ also given for comparison recorded at same scan rate of 0.1 mV s^{-1}. b) Typical galvanostatic charge–discharge curves at current densities of 20 mA g^{-1} (based on cathode loading) in room temperature. Reproduced with permission.[118] Copyright 2013, American Chemical Society. c) CV traces of C-$LiTi_2(PO_4)_3/LiC_6$ cell tested between 1.85–3 V at a scan rate of 0.1 mV s^{-1}. The CV traces of the half-cells, Li/C-$LiTi_2(PO_4)_3$ and Li/Graphite also provided a comparison recorded at same scan rate of 0.1 mV s^{-1}. d) Typical galvanostatic charge–discharge curves of C-$LiTi_2(PO_4)_3/LiC_6$ cells at various current densities (Integer represents the current density in mA cm^{-2} and the capacity has been calculated based on cathode mass loading). Reproduced with permission.[169] Copyright 2014, John Wiley and Sons. e) Typical charge–discharge curves of $LiMn_2O_4/\alpha$-Fe_2O_3 (pre-treated) cell at various current densities between 1.4–3.5 V. f) Rate capability studies of $LiMn_2O_4/\alpha$-Fe_2O_3 (pre-treated) cell with coulombic efficiency, and g) long term cycling profiles with coulombic efficiency. Here, 1 C is assumed to be 1000 mA g^{-1} with respect to anode loading. Reproduced with permission.[168] Copyright 2015, John Wiley and Sons.

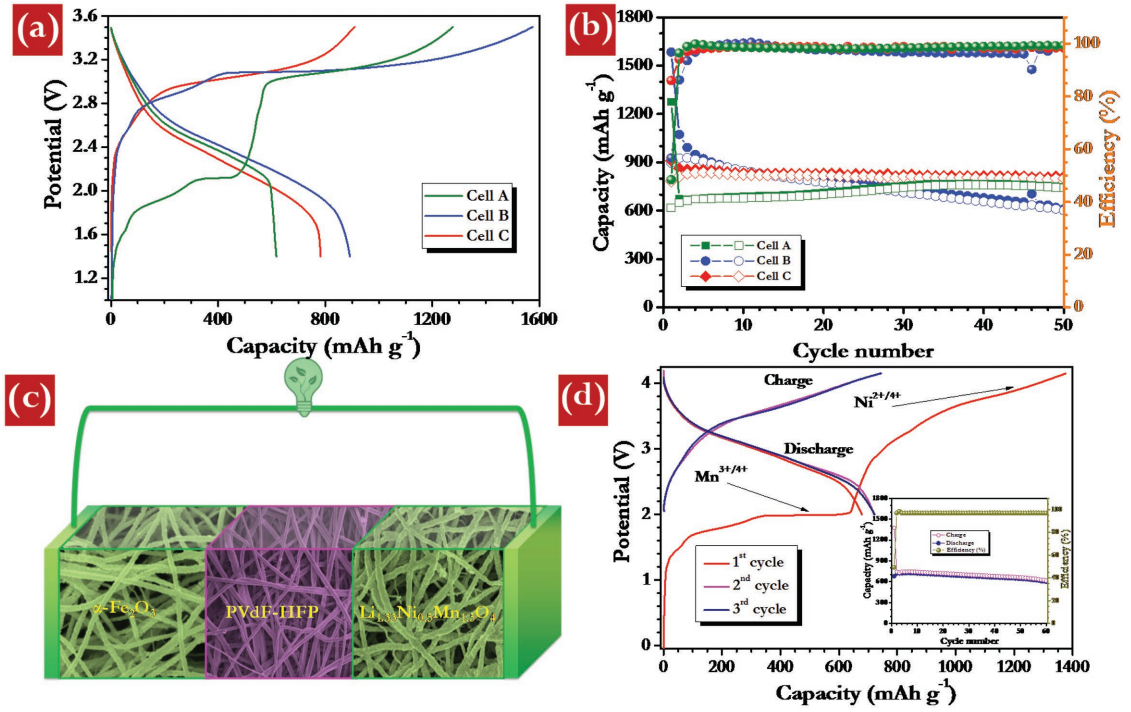

Figure 11. Electrochemical performance of $LiMn_2O_3/\alpha$-Fe_2O_3 full-cell at a current density of 100 mA g^{-1}. Capacity and applied currents are based on anode loading a) typical first charge–discharge curves. Cell A: Pre-lithiated cathode ($Li_{1.26}Mn_2O_4$) is paired with α-Fe_2O_3 by considering the first discharge capacity of the cathode (≈120 mA h g^{-1}) and first charge capacity of anode (≈1282 mA h g^{-1}). Cell B: $LiMn_2O_4/\alpha$-Fe_2O_3 cell has been assembled without any electrode treatment by considering first discharge capacities of both cathode and anode. Cell C: Pre-treated α-Fe_2O_3 has been (tested for two galvanostatic cycles in half-cell assembly at Swagelok configuration) used for the fabrication of full-cell with $LiMn_2O_4$. Here, the first discharge capacity of cathode (≈120 mA h g^{-1}) and second charge capacity of α-Fe_2O_3 (≈1284 mA h g^{-1}) are used for the mass balance. b) Cycling profiles of the three cells and corresponding columbic efficiency. Capacity is based on anode loading. Reproduced with permission.[181] Copyright 2016, Elsevier. c) Schematic representation of typical all 1D Li-ion battery and d) typical charge–discharge curves of $Li_{1.33}Ni_{0.5}Mn_{1.5}O_4$/1 M $LiPF_6$ gelled PVDF-HFP/α-Fe_2O_3 cell between 2 and 4.15 V at current density of 100 mA g^{-1}. Inset: Cycling profiles of $Li_{1.33}Ni_{0.5}Mn_{1.5}O_4$/1 M $LiPF_6$ gelled PVDF-HFP/α-Fe_2O_3 cell between 2 and 4.15 V at current density of 100 mA g^{-1}. The capacity is based on the anode mass loading. Filled and open symbols correspond to charge and discharge, respectively. Reproduced with permission.[182] Copyright 2016, Elsevier.

Although the overlithiation has been carried out for spinel cathodes via a chemical approach with scalability in mind, it influences the morphological features of the resultant phase. Additionally, it is difficult to control the precocious amount of Li-insertion resulting in the need of an additional purification step to remove any solvent impurities. Moreover, ICP studies are required to estimate the exact amount of Li inserted into the cathodes. On the other hand, where an electrochemical approach is concerned, the amount of Li required to compensate the ICL has been precisely controlled and no additional step is required to estimate the amount of Li. Unfortunately, while this procedure cannot be employed for all the cathodes, it is certainly well suited for $LiMn_2O_4$ and its derivative, $Li_3V_2(PO_4)_3$, V_2O_5, and $LiVPO_4F$ cathodes. Aravindan et al.[181] studied the electrochemical activity of α-Fe_2O_3 nanorods with an electrochemically lithiated spinel cathode ($Li_{1.26}Mn_2O_4$). Also, the performance of this configuration is compared with an excess cathode loading and electrochemically pre-treated α-Fe_2O_3 nanofibers assemblies (**Figure 11**). Excellent electrochemical profiles are noted for both electrochemically overlithiated and treated assemblies when compared to excess cathode loading. Furthermore, the same procedure has been extended for the Ni-doped spinel ($LiNi_{0.5}Mn_{1.5}O_4$), in which all the active materials are based on the 1D nanofibers prepared by electrospinning technique.[182].

12. Other Procedures

Apart from the mentioned procedures for the pre-treating/pre-lithiation of electrodes, several other techniques are also explored such as surface modification. Surface modification of active materials with conducting coatings, preferably carbon and metal oxide coatings (e.g., Al_2O_3, TiO_2 etc.), are often claimed for the suppression of ICL when compared to native material.[183] This is one of the nominal procedures used to improve the cyclability and high rate performance of the material irrespective of charge storage mechanism or anode/cathode. This modification certainly improves the cyclability, and effectively prevents the direct contact with an electrolyte solution as well as any unwanted side reactions. As a result, the suppression of ICL is observed, however, the suppression is of small extent only. Still, a significant ICL remains after the surface modification. In such cases, the electrodes must be treated using either of the procedures described above for the complete elimination of ICL.

Short-circuiting is one of the approaches utilized for the pre-lithiation process. Similar to the above process, the working electrode and metallic Li strip is placed in the presence of an electrolyte with a separator. Both terminals are connected by an external circuit with an appropriate load. Based on the desired level of Li, the load and duration is varied. For example, Barker et al.[184] adopted this procedure for the pre-lithiation of hard carbon and subsequently paired it with non-stoichiometric V_6O_{13} as an anode.

Sun et al.[185] reported the possibility of mixing the nanoscopic Co/Li_2O as an additive during the formulation of the $LiFePO_4$ electrodes while pairing it with a graphite anode. The Co/Li_2O is prepared by melting the metallic Li at 185 °C and then reacts with the Co_3O_4, where the temperature subsequently increases to 200 °C to complete the reaction. This process ensures the resultant Co/Li_2O is in the nanosized form. Then, the $LiFePO_4$ based electrode is prepared along with Co/Li_2O in a conventional slurry coating process. On the other hand, micrometer and sub-micrometer sized particulates failed to deliver a similar behavior. As a result, nanosized metal oxides are preferred for this type of additive purpose. This additive is not only used for compensating the ICL, but also translates into better cycling profiles as well. Similarly, Xu et al.[186] explored the Li_5FeO_4 as cathode additive for $LiCoO_2$ when coupled with a hard carbon anode. Apparently, utilization of 4 Li-ions per one mole of Li_5FeO_4 additive will be useful to mitigate the ICL.

Interestingly, some reports are available on the performance of a full-cell without any pre-lithiation procedures. As a result, the full-cell requires a large amount of cathode loading which certainly leads to a significant ICL in the first cycle. Further, this high loading not only affects the net energy density but also the cyclability during a repeated charge–discharge process. For example, Jin et al.[187,188] observed the inferior performance of a multi-layer graphene/Si film and Fe_3O_4/reduced graphene oxide composites with $LiNi_{1/3}Mn_{1/3}Ni_{1/3}O_2$ cathode. Similarly, numerous anodes were explored in the full-cell assembly without any pre-treating procedures. For instance, Fe_2O_3 with $LiFePO_4$[189] and $LiMn_{0.8}Fe_{0.2}PO_4$,[190] Fe_3O_4 with $LiMn_2O_4$,[191] $ZnMn_2O_4$ with $LiMn_{1.5}Ni_{0.5}O_4$[192] and $Li_3Nd_3W_2O_{12}$ with $LiMn_2O_4$[193] were explored.

13. Summary and Outlook

Fabrication of a practical Li-ion cell, i.e., full-cell assembly, is not a straight forward procedure for the case of high capacity anodes that undergo either a conversion or alloying reaction or combination of those two. This type of assembly completely contradicts the fabrication of the traditional "rocking-chair" LIB. This is mainly because of the unusual ICL originating from the electrolyte decomposition and subsequent surface film formation, which in turn provides a large irreversibility during the first cycle. In some cases, the SEI layer formation continues for several cycles. Therefore, various procedures as described above have been adopted to circumvent the ICL issues before the fabrication of full-cell assembly. Although there are few reports available on the usage of such anodes without any pre-treatment and how the lack of pre-treatment eventually leads to the poor cyclability of the cell. Also, the excess de-lithiated cathode phase remains as a dead mass which dilutes the net energy density of the cell. This clearly suggests the importance of pre-treating the electrode is crucial during the paradigm shift from the conventional intercalation process.

A two-step pre-treating method was employed (electrochemical pre-treatment or over lithiated spinel) to mitigate ICL. For example, the anode is discharged and cathode is charged prior to conducting a full-cell assembly. In some cases, the active material is cycled in the half-cell assembly for a few cycles and then paired with a cathode. Alternatively, the working electrode can be placed in a direct contact with metallic Li in the presence of electrolyte (self-discharge method) with a certain amount of applied pressure. As result, a spontaneous thermodynamic reaction triggers the lithiation process. The prime advantages of this technique are the stability and precise control of the amount of Li to be reserved for the compensation of the ICL. Furthermore, attempts have also been made to disperse the active material into the n-butyl Li solution before the formulation of the electrode for the lithiation (chemical lithiation). Previously, the blending of active material with metallic Li (preferably Li strip is placed over working electrode) or Li_3N derivatives has been used. Since the blending of metallic Li experiences practical difficulties, there is a very little research activity being carried out. Also, there will be a possibility of dendritic growth upon the cycling as well, although the usage of the sacrificial salts and artificial SEI are appealing and provide potential scenarios for minimizing the ICL. However, the scalability, gas evolution, toxicity and practical difficulties remain an issue. Hence, those procedures could be interesting for academic aspect, but not useful for the real-time applications.

Very recently, SLMP has been widely used for the mitigation of ICL were metallic Li spheres are covered by a Li_2CO_3 layer. This procedure is similar to placing the metallic Li strip over the electrode, but the presence of a protective Li_2CO_3 layer hinders the direct relationship with electrolyte counterpart. As a result, prohibition of direct contact avoids the unwanted side reactions with an electrolyte. In addition to the spraying of SLMP, activation of such particulates is found appealing and provides some additional improvement in the electrochemical activity.

Chemical lithiation is another scalable approach; however, the estimation of Li must be compromised in order to control the accurate amount of Li inserted and additional cleaning of solvent step. The mentioned setbacks are efficiently tackled from the electrochemical pre-treating step, but the scalability is the main concern. However, the electrochemical pre-lithiation or pre-treating step was well suited for only the laboratory scale studies.

All the techniques proposed for the mitigation of ICL found interesting in academic aspect, but employing for the commercialization is questionable due to time consuming multiple step process and its scalability. Utilizing SLMP is a straightforward and efficient procedure for the elimination of ICL, which can be easily translated in to industrial scale. The only issue with this procedure is the expense. Hence, research activities must be carried out in a cost-effective manner. For instance, Li metal powder prepared through DET. Inclusion of additives such as Li_3N, M/Li_2O, Li_5FeO_4, etc., in the cathodic side is also very promising for mitigating the ICL without compromising

the volumetric capacity and rate performance. Additionally, the approaches and new techniques on this topic are highly appreciated for mitigation of the ICL. This is not only helpful for the LIB applications, also useful for a Li-ion capacitor as well. Therefore, an efficient technique must be highly feasible and scalable for further development and subsequent commercialization, although it offers minor setbacks like (e.g., drop in cell potential, initial reversibility, pre-treating time etc.,), but it can be sacrificed.

By considering the pros and cons in the techniques and procedures mentioned, further research activities must be carried out to develop Li metal powders with stabilized surfaces like Li_2CO_3 in cost effective manner. Further, we certainly believe that usage of stabilized Li metal powder is beneficial for the elimination of large irreversibility in high capacity anodes, irrespective of the charge storage mechanism of anode. In addition, this stabilized Li powder can be efficiently used in both laboratory and industrial scale. Besides the elimination of ICL in negative electrodes, the usage of thin metallic Li as anode for the development of high energy Li-ion power packs are seriously considered for reality in recent past. This stabilized metal powders are certainly useful for the development of such thin metallic anodes with high reversibility owing to its high surface area and limited reactivity with electrolyte. Apparently, the stabilized Li metal powder certainly holds the promising future to solve one of the fundamental issue of ICL in Li-ion batteries. Also, this stabilized powder could be used as metallic anode for the development of shape versatile Li-ion power packs.

Acknowledgements

This work was financially supported by NTU-HUJ Create Phase II which is a joint research programme between the Hebrew University of Jerusalem (HUJ, Israel) and Nanyang Technological University (NTU, Singapore) with CREATE (Campus for Research Excellence and Technological Enterprise) funding from National Research Foundation of Singapore (NRF, Singapore). YSL acknowledges the finacial support from the National Research Foundation of Korea (NRF) grant funded by the Korean government (Ministry of Science, ICT & Future Planning) (No. 2016R1A4A1012224).

Keywords

anodes, irreversible capacity loss, Li-ion batteries, solid electrolyte interface

Received: November 24, 2016
Revised: February 9, 2017
Published online:

[1] F. Schipper, D. Aurbach, *Russ. J. Electrochem.* **2016**, *52*, 1095.
[2] E. M. Erickson, C. Ghanty, D. Aurbach, *J. Phys. Chem. Lett.* **2014**, *5*, 3313.
[3] M. Armand, J.-M. Tarascon, *Nature* **2008**, *451*, 652.
[4] J. M. Tarascon, M. Armand, *Nature* **2001**, *414*, 359.
[5] V. Aravindan, Y.-S. Lee, S. Madhavi, *Adv. Energy Mater.* **2015**, *5*, 1402225.
[6] N. Nitta, F. Wu, J. T. Lee, G. Yushin, *Mater. Today* **2015**, *18*, 252.
[7] V. Aravindan, Y.-S. Lee, R. Yazami, S. Madhavi, *Mater. Today* **2015**, *18*, 345.
[8] V. Aravindan, J. Sundaramurthy, P. Suresh Kumar, Y.-S. Lee, S. Ramakrishna, S. Madhavi, *Chem. Commun.* **2015**, *51*, 2225.
[9] V. Aravindan, J. Gnanaraj, S. Madhavi, H.-K. Liu, *Chem. Eur. J.* **2011**, *17*, 14326.
[10] V. Aravindan, J. Gnanaraj, Y.-S. Lee, S. Madhavi, *J. Mater. Chem. A* **2013**, *1*, 3518.
[11] V. Aravindan, M. Ulaganathan, S. Madhavi, *J. Mater. Chem. A* **2016**, *4*, 7538.
[12] H. D. Yoo, E. Markevich, G. Salitra, D. Sharon, D. Aurbach, *Mater. Today* **2014**, *17*, 110.
[13] M. M. Thackeray, C. Wolverton, E. D. Isaacs, *Energy Environ. Sci.* **2012**, *5*, 7854.
[14] V. Aravindan, J. Gnanaraj, Y.-S. Lee, S. Madhavi, *Chem. Rev.* **2014**, *114*, 11619.
[15] A. D. W. Todd, P. P. Ferguson, M. D. Fleischauer, J. R. Dahn, *Int. J. Energy Res.* **2010**, *34*, 535.
[16] K. Xu, *Chem. Rev.* **2004**, *104*, 4303.
[17] M. V. Reddy, G. V. Subba Rao, B. V. R. Chowdari, *Chem. Rev.* **2013**, *113*, 5364.
[18] N.-S. Choi, Z. Chen, S. A. Freunberger, X. Ji, Y.-K. Sun, K. Amine, G. Yushin, L. F. Nazar, J. Cho, P. G. Bruce, *Angew. Chem. Int. Ed.* **2012**, *51*, 9994.
[19] V. Etacheri, R. Marom, R. Elazari, G. Salitra, D. Aurbach, *Energy Environ. Sci.* **2011**, *4*, 3243.
[20] H. Bryngelsson, M. Stjerndahl, T. Gustafsson, K. Edström, *J. Power Sources* **2007**, *174*, 970.
[21] K. Edström, M. Herstedt, D. P. Abraham, *J. Power Sources* **2006**, *153*, 380.
[22] D. Aurbach, M. D. Levi, E. Levi, A. Schechter, *J. Phys. Chem. B* **1997**, *101*, 2195.
[23] N. A. Kaskhedikar, J. Maier, *Adv. Mater.* **2009**, *21*, 2664.
[24] K. Xu, *Chem. Rev.* **2014**, *114*, 11503.
[25] X.-B. Cheng, R. Zhang, C.-Z. Zhao, F. Wei, J.-G. Zhang, Q. Zhang, *Adv. Sci.* **2016**, *3*, 1500213.
[26] P. Verma, P. Maire, P. Novák, *Electrochim. Acta* **2010**, *55*, 6332.
[27] T. L. Kulova, A. M. Skundin, *J. Solid State Electrochem.* **2003**, *8*, 59.
[28] T. L. Kulova, A. M. Skundin, *Russ. J. Electrochem.* **2010**, *46*, 470.
[29] T. L. Kulova, *Russ. J. Electrochem.* **2011**, *47*, 965.
[30] T. L. Kulova, A. M. Skundin, Y. V. Pleskov, E. I. Terukov, O. I. Kon'kov, *J. Electroanal. Chem.* **2007**, *600*, 217.
[31] N. Dimov, Y. Xia, M. Yoshio, *J. Power Sources* **2007**, *171*, 886.
[32] H. Sun, X. He, J. Ren, J. Li, C. Jiang, C. Wan, *Electrochim. Acta* **2007**, *52*, 4312.
[33] M. S. Park, W. Y. Yoon, *J. Power Sources* **2003**, *114*, 237.
[34] S. W. Kim, Y. J. Ahn, W. Y. Yoon, *Met. Mater.* **2000**, *6*, 345.
[35] S.-T. Hong, J.-S. Kim, S.-J. Lim, W. Y. Yoon, *Electrochim. Acta* **2004**, *50*, 535.
[36] B. M. Song, H. E. Park, W. Y. Yoon, *J. Kor. Phys. Soc.* **2009**, *54*, 1136.
[37] J. H. Lee, C. W. Lim, J. K. Lee, S. M. Cho, B. K. Kim, W. Y. Yoon, *Electrochim. Acta* **2014**, *131*, 202.
[38] W.-S. Kim, W.-Y. Yoon, *Electrochim. Acta* **2004**, *50*, 541.
[39] I. W. Seong, K. T. Kim, W. Y. Yoon, *J. Power Sources* **2009**, *189*, 511.
[40] B. Xiang, L. Wang, G. Liu, A. M. Minor, *J. Electrochem. Soc.* **2013**, *160*, A415.
[41] J. T. Vaughey, G. Liu, J.-G. Zhang, *MRS Bulletin* **2014**, *39*, 429.
[42] Y. Li, B. Fitch, *Electrochem. Commun.* **2011**, *13*, 664.
[43] B. B. Fitch, M. Yakovleva, Y. Li, I. Plitz, A. Skrzypczak, F. Badway, G. G. Amatucci, Y. Gao, *ECS Trans.* **2007**, *3*, 15.
[44] C. R. Jarvis, M. J. Lain, Y. Gao, M. Yakovleva, *J. Power Sources* **2005**, *146*, 331.
[45] C. R. Jarvis, M. J. Lain, M. V. Yakovleva, Y. Gao, *J. Power Sources* **2006**, *162*, 800.

[46] S. Brutti, V. Gentili, P. Reale, L. Carbone, S. Panero, *J. Power Sources* **2011**, *196*, 9792.
[47] H. Zhang, X. Sun, X. Huang, L. Zhou, *Nanoscale* **2015**, *7*, 3270.
[48] M. W. Forney, M. J. Ganter, J. W. Staub, R. D. Ridgley, B. J. Landi, *Nano Lett.* **2013**, *13*, 4158.
[49] H. Zhao, Z. Wang, P. Lu, M. Jiang, F. Shi, X. Song, Z. Zheng, X. Zhou, Y. Fu, G. Abdelbast, X. Xiao, Z. Liu, V. S. Battaglia, K. Zaghib, G. Liu, *Nano Lett.* **2014**, *14*, 6704.
[50] X.-L. Wang, W.-Q. Han, H. Chen, J. Bai, T. A. Tyson, X.-Q. Yu, X.-J. Wang, X.-Q. Yang, *J. Am. Chem. Soc.* **2011**, *133*, 20692.
[51] Z. Wang, Y. Fu, Z. Zhang, S. Yuan, K. Amine, V. Battaglia, G. Liu, *J. Power Sources* **2014**, *260*, 57.
[52] T. A. Yersak, S.-B. Son, J. S. Cho, S.-S. Suh, Y.-U. Kim, J.-T. Moon, K. H. Oh, S.-H. Lee, *J. Electrochem. Soc.* **2013**, *160*, A1497.
[53] L. Wang, Y. Fu, V. S. Battaglia, G. Liu, *RSC Adv.* **2013**, *3*, 15022.
[54] L. Hu, K. Amine, Z. Zhang, *Electrochem. Commun.* **2014**, *44*, 34.
[55] S. Zheng, Y. Chen, Y. Xu, F. Yi, Y. Zhu, Y. Liu, J. Yang, C. Wang, *Acs Nano* **2013**, *7*, 10995.
[56] K.-W. Nam, S.-B. Ma, W.-S. Yoon, X.-Q. Yang, K.-B. Kim, *Electrochem. Commun.* **2009**, *11*, 1166.
[57] W. J. Cao, M. Greenleaf, Y. X. Li, D. Adams, M. Hagen, T. Doung, J. P. Zheng, *J. Power Sources* **2015**, *280*, 600.
[58] W. J. Cao, J. P. Zheng, *J. Electrochem. Soc.* **2013**, *160*, A1572.
[59] W. Cao, Y. Li, B. Fitch, J. Shih, T. Doung, J. Zheng, *J. Power Sources* **2014**, *268*, 841.
[60] J. Zhao, Z. Lu, N. Liu, H.-W. Lee, M. T. McDowell, Y. Cui, *Nat. Commun.* **2014**, *5*, Art. No. 5088.
[61] J. Zhao, H.-W. Lee, J. Sun, K. Yan, Y. Liu, W. Liu, Z. Lu, D. Lin, G. Zhou, Y. Cui, *Proc. Nat. Acad. Sci. USA* **2016**, *113*, 7408.
[62] D. Shanmukaraj, S. Grugeon, S. Laruelle, G. Douglade, J.-M. Tarascon, M. Armand, *Electrochem. Commun.* **2010**, *12*, 1344.
[63] D. H. Gregory, *Chem. Record* **2008**, *8*, 229.
[64] Z. Wen, K. Wang, L. Chen, J. Xie, *Electrochem. Commun.* **2006**, *8*, 1349.
[65] T. A. Yersak, J. E. Trevey, S.-H. Lee, *J. Power Sources* **2011**, *196*, 9830.
[66] G. G. Amatucci, N. Pereira, F. Badway, M. Sina, F. Cosandey, M. Ruotolo, C. Cao, *J. Fluorine Chem.* **2011**, *132*, 1086.
[67] K. Park, B.-C. Yu, J. B. Goodenough, *Adv. Energy Mater.* **2016**, *6*, 1502534.
[68] M. Nishijima, T. Kagohashi, M. Imanishi, Y. Takeda, O. Yamamoto, S. Kondo, *Solid State Ionics* **1996**, *83*, 107.
[69] T. Shodai, S. Okada, S.-i. Tobishima, J.-i. Yamaki, *Solid State Ionics* **1996**, *86–88*, Part 2, 785.
[70] T. Shodai, S. Okada, S. Tobishima, J. Yamaki, *J. Power Sources* **1997**, *68*, 515.
[71] Y. Takeda, M. Nishijima, M. Yamahata, K. Takeda, N. Imanishi, O. Yamamoto, *Solid State Ionics* **2000**, *130*, 61.
[72] T. Shodai, Y. Sakurai, T. Suzuki, *Solid State Ionics* **1999**, *122*, 85.
[73] M. Nishijima, T. Kagohashi, Y. Takeda, M. Imanishi, O. Yamamoto, *J. Power Sources* **1997**, *68*, 510.
[74] J. Yang, K. Wang, J. Xie, *J. Electrochem. Soc.* **2003**, *150*, A140.
[75] Y.-M. Kang, S.-C. Park, Y.-S. Kang, P. S. Lee, J.-Y. Lee, *Solid State Ionics* **2003**, *156*, 263.
[76] K. Wang, J. Yang, J. Xie, S. Zhang, *Solid State Ionics* **2003**, *160*, 69.
[77] Y. Liu, T. Matsumura, N. Imanishi, T. Ichikawa, A. Hirano, Y. Takeda, *Electrochem. Commun.* **2004**, *6*, 632.
[78] Y. Liu, K. Horikawa, M. Fujiyosi, N. Imanishi, A. Hirano, Y. Takeda, *J. Electrochem. Soc.* **2004**, *151*, A1450.
[79] D. Liu, S. Zhan, G. Chen, W. Pan, C. Wang, Y. Wei, *Mater. Lett.* **2008**, *62*, 4210.
[80] D. Liu, F. Du, W. Pan, G. Chen, C. Wang, Y. Wei, *Mater. Lett.* **2009**, *63*, 504.
[81] Y. Liu, K. Horikawa, M. Fujiyosi, N. Imanishi, A. Hirano, Y. Takeda, *Electrochim. Acta* **2004**, *49*, 3487.
[82] K. Hanai, Y. Liu, T. Matsumura, N. Imanishi, A. Hirano, Y. Takeda, *Solid State Ionics* **2008**, *179*, 1725.
[83] H. Sun, X. He, J. Li, J. Ren, C. Y. Jiang, C. Wan, *Solid State Ionics* **2006**, *177*, 1331.
[84] Y. Liu, K. Hanai, K. Horikawa, N. Imanishi, A. Hirano, Y. Takeda, *Mater. Chem. Phys.* **2005**, *89*, 80.
[85] J. Yang, Y. Takeda, N. Imanishi, T. Ichikawa, O. Yamamoto, *Solid State Ionics* **2000**, *135*, 175.
[86] J. Yang, Y. Takeda, Q. Li, N. Imanishi, O. Yamamoto, *J. Power Sources* **2000**, *90*, 64.
[87] J. Yang, Y. Takeda, N. Imanishi, O. Yamamoto, *J. Electrochem. Soc.* **2000**, *147*, 1671.
[88] J. Yang, Y. Takeda, Q. Li, N. Imanishi, O. Yamamoto, *J. Power Sources* **2001**, *97–98*, 779.
[89] Y. Takeda, J. Yang, *J. Power Sources* **2001**, *97–98*, 244.
[90] Y. Liu, Y. Takeda, T. Matsumura, J. Yang, N. Imanishi, A. Hirano, O. Yamamoto, *J. Electrochem. Soc.* **2006**, *153*, A437.
[91] Y. Takeda, J. Yang, N. Imanishi, *Solid State Ionics* **2002**, *152–153*, 35.
[92] J. Yang, Y. Takeda, C. Capiglia, X. D. Liu, N. Imanishi, O. Yamamoto, *J. Power Sources* **2003**, *119–121*, 56.
[93] J. Yang, Y. Takeda, N. Imanishi, O. Yamamoto, *Electrochim. Acta* **2001**, *46*, 2659.
[94] J. Yang, Y. Takeda, N. Imanishi, J. Y. Xie, O. Yamamoto, *J. Power Sources* **2001**, *97–98*, 216.
[95] Y. Liu, J. Yang, N. Imanishi, A. Hirano, Y. Takeda, O. Yamamoto, *J. Power Sources* **2005**, *146*, 376.
[96] Y. Liu, K. Horikawa, M. Fujiyoshi, T. Matsumura, N. Imanishi, Y. Takeda, *Solid State Ionics* **2004**, *172*, 69.
[97] A. K. Rai, J. Lim, V. Mathew, J. Gim, J. Kang, B. J. Paul, D. Kim, S. Ahn, S. Kim, K. Ahn, J. Kim, *Electrochem. Commun.* **2012**, *19*, 9.
[98] Y. Takeda, N. Imanishi, O. Yamamoto, *Electrochemistry* **2009**, *77*, 784.
[99] S. Menkin, D. Golodnitsky, E. Peled, *Electrochem. Commun.* **2009**, *11*, 1789.
[100] Z. Sheng Shui, *J. Power Sources* **2006**, *162*, 1379.
[101] N.-W. Li, Y.-X. Yin, C.-P. Yang, Y.-G. Guo, *Adv. Mater.* **2016**, *28*, 1853.
[102] J. Zhao, Z. Lu, H. Wang, W. Liu, H.-W. Lee, K. Yan, D. Zhuo, D. Lin, N. Liu, Y. Cui, *J. Am. Chem. Soc.* **2015**, *137*, 8372.
[103] H. Guk, D. Kim, S.-H. Choi, D. H. Chung, S. S. Han, *J. Electrochem. Soc.* **2016**, *163*, A917.
[104] M. B. Dines, *Mat. Res. Bull.* **1975**, *10*, 287.
[105] J. M. Cocciantelli, J. P. Doumerc, M. Pouchard, M. Broussely, J. Labat, *J. Power Sources* **1991**, *34*, 103.
[106] Y. L. Cheah, V. Aravindan, S. Madhavi, *J. Electrochem. Soc.* **2013**, *160*, A1016.
[107] J. M. Coccíantelli, M. Ménétrier, C. Delmas, J. P. Doumerc, M. Pouchard, P. Hagenmuller, *Solid State Ionics* **1992**, *50*, 99.
[108] A. Manthiram, Y. Fu, S.-H. Chung, C. Zu, Y.-S. Su, *Chem. Rev.* **2014**, *114*, 11751.
[109] C. S. Johnson, D. W. Dees, M. F. Mansuetto, M. M. Thackeray, D. R. Vissers, D. Argyriou, C. K. Loong, L. Christensen, *J. Power Sources* **1997**, *68*, 570.
[110] L. Q. Mai, B. Hu, W. Chen, Y. Y. Qi, C. S. Lao, R. S. Yang, Y. Dai, Z. L. Wang, *Adv. Mater.* **2007**, *19*, 3712.
[111] L. Mai, L. Xu, B. Hu, Y. Gu, *J. Mat. Res.* **2010**, *25*, 1413.
[112] L. Q. Mai, Y. Gao, J. G. Guan, B. Hu, L. Xu, W. Jin, *Int. J. Energy Res.* **2009**, *4*, 755.
[113] C. Delmas, S. Brèthes, M. Ménétrier, *J. Power Sources* **1991**, *34*, 113.
[114] B. Garcia, M. Millet, J. P. Pereira-Ramos, N. Baffier, D. Bloch, *J. Power Sources* **1999**, *81–82*, 670.
[115] N. A. Chernova, M. Roppolo, A. C. Dillon, M. S. Whittingham, *J. Mater. Chem.* **2009**, *19*, 2526.

[116] M. S. Whittingham, M. B. Dines, *J. Electrochem. Soc.* **1977**, *124*, 1387.
[117] M. G. Scott, A. H. Whitehead, J. R. Owen, *J. Electrochem. Soc.* **1998**, *145*, 1506.
[118] Y. L. Cheah, V. Aravindan, S. Madhavi, *ACS Appl. Mater. Interfaces* **2013**, *5*, 3475.
[119] N. Liu, L. Hu, M. T. McDowell, A. Jackson, Y. Cui, *ACS Nano* **2011**, *5*, 6487.
[120] J. Hassoun, K.-S. Lee, Y.-K. Sun, B. Scrosati, *J. Am. Chem. Soc.* **2011**, *133*, 3139.
[121] G. A. Elia, J. Wang, D. Bresser, J. Li, B. Scrosati, S. Passerini, J. Hassoun, *ACS Appl. Mater. Interfaces* **2014**, *6*, 12956.
[122] O. Vargas, Á. Caballero, J. Morales, *Electrochim. Acta* **2014**, *130*, 551.
[123] C. Chae, H.-J. Noh, J. K. Lee, B. Scrosati, Y.-K. Sun, *Adv. Funct. Mater.* **2014**, *24*, 3036.
[124] S. Brutti, J. Hassoun, B. Scrosati, C.-Y. Lin, H. Wu, H.-W. Hsieh, *J. Power Sources* **2012**, *217*, 72.
[125] J. Hassoun, D.-J. Lee, Y.-K. Sun, B. Scrosati, *Solid State Ionics* **2011**, *202*, 36.
[126] J. Hassoun, S. Panero, P. Reale, B. Scrosati, *Adv. Mater.* **2009**, *21*, 4807.
[127] F. Croce, M. L. Focarete, J. Hassoun, I. Meschini, B. Scrosati, *Energy Environ. Sci.* **2011**, *4*, 921.
[128] J. Hassoun, A. Fernicola, M. A. Navarra, S. Panero, B. Scrosati, *J. Power Sources* **2010**, *195*, 574.
[129] S.-K. Lee, S.-M. Oh, E. Park, B. Scrosati, J. Hassoun, M.-S. Park, Y.-J. Kim, H. Kim, I. Belharouak, Y.-K. Sun, *Nano Lett.* **2015**, *15*, 2863.
[130] J.-S. Bridel, S. Grugeon, S. Laruelle, J. Hassoun, P. Reale, B. Scrosati, J.-M. Tarascon, *J. Power Sources* **2010**, *195*, 2036.
[131] M. Agostini, J. Hassoun, J. Liu, M. Jeong, H. Nara, T. Momma, T. Osaka, Y.-K. Sun, B. Scrosati, *ACS Appl. Mater. Interfaces* **2014**, *6*, 10924.
[132] J. Hassoun, H.-G. Jung, D.-J. Lee, J.-B. Park, K. Amine, Y.-K. Sun, B. Scrosati, *Nano Lett.* **2012**, *12*, 5775.
[133] J. Hassoun, P. Reale, S. Panero, B. Scrosati, M. Wachtler, M. Fleischhammer, M. Kasper, M. Wohlfahrt-Mehrens, *Electrochim. Acta* **2010**, *55*, 4194.
[134] M. Agostini, B. Scrosati, J. Hassoun, *Adv. Energy Mater.* **2015**, *5*, 1500481.
[135] G. A. Elia, F. Nobili, R. Tossici, R. Marassi, A. Savoini, S. Panero, J. Hassoun, *J. Power Sources* **2015**, *275*, 227.
[136] D. Di Lecce, S. Brutti, S. Panero, J. Hassoun, *Mater. Lett.* **2015**, *139*, 329.
[137] M. Agostini, J. Hassoun, *Sci. Rep.* **2014**, *5*, Article number: 7591.
[138] Ó. Vargas, Á. Caballero, J. Morales, E. Rodríguez-Castellón, *ACS Appl. Mater. Interfaces* **2014**, *6*, 3290.
[139] Ó. Vargas, Á. Caballero, J. Morales, *Electrochim. Acta* **2015**, *165*, 365.
[140] J. Hassoun, F. Bonaccorso, M. Agostini, M. Angelucci, M. G. Betti, R. Cingolani, M. Gemmi, C. Mariani, S. Panero, V. Pellegrini, B. Scrosati, *Nano Lett.* **2014**, *14*, 4901.
[141] P. Xiong, L. Peng, D. Chen, Y. Zhao, X. Wang, G. Yu, *Nano Energy* **2015**, *12*, 816.
[142] Y. Wang, G. Xing, Z. J. Han, Y. Shi, J. I. Wong, Z. X. Huang, K. Ostrikov, H. Y. Yang, *Nanoscale* **2014**, *6*, 8884.
[143] G.-L. Xu, Y.-F. Xu, J.-C. Fang, F. Fu, H. Sun, L. Huang, S. Yang, S.-G. Sun, *ACS Appl. Mater. Interfaces* **2013**, *5*, 6316.
[144] H. Ming, J. Ming, S.-M. Oh, S. Tian, Q. Zhou, H. Huang, Y.-K. Sun, J. Zheng, *ACS Appl. Mater. Interfaces* **2014**, *6*, 15499.
[145] J. Ming, W. J. Kwak, S. J. Youn, H. Ming, J. Hassoun, Y.-K. Sun, *Energy Technol.* **2014**, *2*, 778.
[146] H. Ming, J. Ming, W.-J. Kwak, W. Yang, Q. Zhou, J. Zheng, Y.-K. Sun, *Electrochim. Acta* **2015**, *169*, 291.
[147] J. Hassoun, J. Kim, D.-J. Lee, H.-G. Jung, S.-M. Lee, Y.-K. Sun, B. Scrosati, *J. Power Sources* **2012**, *202*, 308.
[148] F. Bonino, S. Brutti, P. Reale, B. Scrosati, L. Gherghel, J. Wu, K. Müllen, *Adv. Mater.* **2005**, *17*, 743.
[149] A. Caballero, L. Hernán, J. Morales, *ChemSusChem* **2011**, *4*, 658.
[150] J. Hassoun, F. Croce, I. Hong, B. Scrosati, *Electrochem. Commun.* **2011**, *13*, 228.
[151] G. Derrien, J. Hassoun, S. Panero, B. Scrosati, *Adv. Mater.* **2007**, *19*, 2336.
[152] R. Elazari, G. Salitra, G. Gershinsky, A. Garsuch, A. Panchenko, D. Aurbach, *Electrochem. Commun.* **2012**, *14*, 21.
[153] K. Fridman, R. Sharabi, R. Elazari, G. Gershinsky, E. Markevich, G. Salitra, D. Aurbach, A. Garsuch, J. Lampert, *Electrochem. Commun.* **2013**, *33*, 31.
[154] R. Elazari, G. Salitra, G. Gershinsky, A. Garsuch, A. Panchenko, D. Aurbach, *J. Electrochem. Soc.* **2012**, *159*, A1440.
[155] R. Verrelli, J. Hassoun, A. Farkas, T. Jacob, B. Scrosati, *J. Mater. Chem. A* **2013**, *1*, 15329.
[156] R. Verrelli, B. Scrosati, Y.-K. Sun, J. Hassoun, *ACS Appl. Mater. Interfaces* **2014**, *6*, 5206.
[157] R. Verrelli, R. Brescia, A. Scarpellini, L. Manna, B. Scrosati, J. Hassoun, *RSC Adv.* **2014**, *4*, 61855.
[158] R. Verrelli, J. Hassoun, *ChemElectroChem.* **2015**, *2*, 988.
[159] A. Suryawanshi, V. Aravindan, D. Mhamane, P. Yadav, S. Patil, S. Madhavi, S. Ogale, *Energy Storage Mater.* **2015**, *1*, 152.
[160] A. Suryawanshi, V. Aravindan, S. Madhavi, S. Ogale, *ChemSusChem* **2016**, *9*, 2193.
[161] C. Chae, H. Park, D. Kim, J. Kim, E.-S. Oh, J. K. Lee, *J. Power Sources* **2013**, *244*, 214.
[162] G. A. Elia, S. Panero, A. Savoini, B. Scrosati, J. Hassoun, *Electrochim. Acta* **2013**, *90*, 690.
[163] J. Hassoun, G. Mulas, S. Panero, B. Scrosati, *Electrochem. Commun.* **2007**, *9*, 2075.
[164] J. Hassoun, S. Panero, G. Mulas, B. Scrosati, *J. Power Sources* **2007**, *171*, 928.
[165] O. Vargas, A. Caballero, J. Morales, G. A. Elia, B. Scrosati, J. Hassoun, *Phys. Chem. Chem. Phys.* **2013**, *15*, 20444.
[166] Y. Wang, Y. Wang, D. Jia, Z. Peng, Y. Xia, G. Zheng, *Nano Lett.* **2014**, *14*, 1080.
[167] A. Varzi, D. Bresser, J. von Zamory, F. Müller, S. Passerini, *Adv. Energy Mater.* **2014**, *4*, 1400054.
[168] S. Jayaraman, V. Aravindan, M. Ulaganathan, W. C. Ling, S. Ramakrishna, S. Madhavi, *Adv. Sci.* **2015**, *2*, 1500050.
[169] V. Aravindan, M. Ulaganathan, W. C. Ling, S. Madhavi, *ChemElectroChem.* **2015**, *2*, 231.
[170] S. Jayaraman, V. Aravindan, N. Shubha, M. Ulaganathan, S. Madhavi, *Particle* **2016**, *33*, 306.
[171] J. M. Tarascon, D. Guyomard, *J. Electrochem. Soc.* **1991**, *138*, 2864.
[172] D. Peramunage, K. M. Abraham, *J. Electrochem. Soc.* **1998**, *145*, 1131.
[173] S. Jayaraman, V. Aravindan, P. Suresh Kumar, W. C. Ling, S. Ramakrishna, S. Madhavi, *Chem. Commun.* **2013**, *49*, 6677.
[174] M. C. Kim, K.-W. Nam, E. Hu, X.-Q. Yang, H. Kim, K. Kang, V. Aravindan, W.-S. Kim, Y.-S. Lee, *ChemSusChem* **2014**, *7*, 829.
[175] N. Arun, V. Aravindan, S. Jayaraman, N. Shubha, W. C. Ling, S. Ramakrishna, S. Madhavi, *Nanoscale* **2014**, *6*, 8926.
[176] N. Arun, V. Aravindan, W. C. Ling, S. Madhavi, *J. Power Sources* **2015**, *280*, 240.
[177] N. Arun, A. Jain, V. Aravindan, S. Jayaraman, W. Chui Ling, M. P. Srinivasan, S. Madhavi, *Nano Energy* **2015**, *12*, 69.
[178] F. Badway, I. Plitz, S. Grugeon, S. Laruelle, M. Dollé, A. S. Gozdz, J.-M. Tarascon, *Electrochem. Solid-State Lett.* **2002**, *5*, A115.
[179] P. Poizot, S. Laruelle, S. Grugeon, L. Dupont, J. M. Tarascon, *J. Power Sources* **2001**, *97–98*, 235.

[180] Z. Moorhead-Rosenberg, E. Allcorn, A. Manthiram, *Chem. Mater.* **2014**, *26*, 5905.
[181] V. Aravindan, S. Nan, M. Keppeler, S. Madhavi, *Electrochim. Acta* **2016**, *208*, 225.
[182] V. Aravindan, N. Arun, N. Shubha, J. Sundaramurthy, S. Madhavi, *Electrochim. Acta* **2016**, *215*, 647.
[183] J.-G. Ren, Q.-H. Wu, G. Hong, W.-J. Zhang, H. Wu, K. Amine, J. Yang, S.-T. Lee, *Energy Technol.* **2013**, *1*, 77.
[184] J. Barker, J. Swoyer, M. Y. Saidi, *Electrochem. Soc. Proc.* **1997**, *97-98*, 241.
[185] Y. Sun, H.-W. Lee, Z. W. Seh, N. Liu, J. Sun, Y. Li, Y. Cui, *Nat. Energy* **2016**, *1*, 15008.
[186] X. Su, C. Lin, X. Wang, V. A. Maroni, Y. Ren, C. S. Johnson, W. Lu, *J. Power Sources* **2016**, *324*, 150.
[187] L. Ji, Z. Tan, T. R. Kuykendall, S. Aloni, S. Xun, E. Lin, V. Battaglia, Y. Zhang, *Phys. Chem. Chem. Phys.* **2011**, *13*, 7170.
[188] L. Ji, H. Zheng, A. Ismach, Z. Tan, S. Xun, E. Lin, V. Battaglia, V. Srinivasan, Y. Zhang, *Nano Energy* **2012**, *1*, 164.
[189] K. Cao, L. Jiao, H. Liu, Y. Liu, Y. Wang, Z. Guo, H. Yuan, *Adv. Energy Mater.* **2014**, *5*, 1401421.
[190] S. Hariharan, V. Ramar, S. P. Joshi, P. Balaya, *RSC Adv.* **2013**, *3*, 6386.
[191] X. Fan, J. Shao, X. Xiao, L. Chen, X. Wang, S. Li, H. Ge, *J. Mater. Chem. A* **2014**, *2*, 14641.
[192] F. M. Courtel, H. Duncan, Y. Abu-Lebdeh, I. J. Davidson, *J. Mater. Chem.* **2011**, *21*, 10206.
[193] R. Satish, V. Aravindan, W. C. Ling, J. B. Goodenough, S. Madhavi, *Adv. Energy Mater.* **2014**, *4*, 1301715.